



Lawrence Berkeley Laboratory

UNIVERSITY OF CALIFORNIA

EARTH SCIENCES DIVISION

To be presented at the 1990 SPE California
Regional Meeting, Ventura, CA, April 4-6, 1990,
and to be published in the Proceedings

Flow and Displacement of Bingham Non-Newtonian Fluids in Porous Media

Y.-S. Wu, K. Pruess, and P.A. Witherspoon

January 1990



1 LOAN COPY 1
1 CIRCULATES 1
1 FOR 2 WEEKS 1

Bldg. 50 Library.
Copy 2

LBL-28340

DISCLAIMER

This document was prepared as an account of work sponsored by the United States Government. While this document is believed to contain correct information, neither the United States Government nor any agency thereof, nor the Regents of the University of California, nor any of their employees, makes any warranty, express or implied, or assumes any legal responsibility for the accuracy, completeness, or usefulness of any information, apparatus, product, or process disclosed, or represents that its use would not infringe privately owned rights. Reference herein to any specific commercial product, process, or service by its trade name, trademark, manufacturer, or otherwise, does not necessarily constitute or imply its endorsement, recommendation, or favoring by the United States Government or any agency thereof, or the Regents of the University of California. The views and opinions of authors expressed herein do not necessarily state or reflect those of the United States Government or any agency thereof or the Regents of the University of California.

LBL-28340

Flow and Displacement of Bingham Non-Newtonian Fluids in Porous Media

Y.-S. Wu, K. Pruess, and P. A. Witherspoon

Earth Sciences Division
Lawrence Berkeley Laboratory
University of California
Berkeley, California 94720

January 1990

This work was supported by the Director, Office of Energy Research, Office of Basic Energy Sciences, Engineering and Geosciences Division, of the U.S. Department of Energy under Contract No. DE-AC03-76SF00098.

SPE 20051

Flow and Displacement of Bingham Non-Newtonian Fluids in Porous Media

by Y. -S. Wu, K. Pruess and P. A. Witherspoon, Lawrence Berkeley Laboratories

Abstract

There is considerable evidence that the flow of heavy oil in some reservoirs is non-Newtonian and that this behavior can be approximated by a Bingham type fluid. Investigations in the Laboratory and in a few field tests have shown a behavior that is characteristic of a Bingham fluid; the flow of the heavy oil takes place only after the applied pressure gradient exceeds a certain minimum value. Despite the research that has been carried out over the past 20 years on the flow of non-Newtonian fluids in porous media, very little work has been done on single- and multiple-phase flow of Bingham fluids. At present, there is no reliable method of analyzing pressure buildup data from well tests where the reservoir contains a Bingham oil.

This work presents a theoretical study of the flow and displacement of a Bingham type fluid in porous media. An integral method of analyzing the single phase flow of this type of fluid has been developed. An approximate analytical solution has been obtained for transient flow problems, and its accuracy is confirmed by comparison with numerical solutions. The flow behavior of a slightly-compressible Bingham fluid is discussed, and a new method of well test analysis has been developed by using the integral solution.

To obtain some understanding of the physics of immiscible displacement with Bingham fluids, a Buckley-Leverett type analytical solution with a practical graphic evaluation method has been developed and applied to the problem of displacing a Bingham-type fluid by water. The results reveal how the saturation profile and the displacement efficiency are controlled not only by the relative permeabilities, as in the case of Newtonian fluids, but also by the inherent complexities of Bingham non-Newtonian behavior. In particular, we find that in the displacement process with a Bingham fluid, there exists a limiting maximum saturation, beyond which no further displacement can be achieved.

1. Introduction

Flow of non-Newtonian fluids through porous media is encountered in many subsurface systems involving underground natural resource recovery or storage projects. In the past three decades, a tremendous effort has been expended in developing quantitative analysis of flow of non-Newtonian fluids through porous media. Considerable progress has been reported and much information is available in the chemical engineering, rheology and petroleum engineering literature regarding non-Newtonian fluid flow through porous media (Savins, 1969; Gogarty, 1967; van Poolen, 1969; Ikoku and Ramey, 1979; Odeh and Yang, 1979). The theoretical investigations carried out in this field have mainly concentrated on single-phase power-law non-Newtonian fluid flow, while the experimental studies have intended to provide rheological models for non-Newtonian fluids and porous materials of interest.

There is considerable evidence from laboratory experiments and field tests that certain fluids in porous media exhibit a Bingham-type non-Newtonian behavior (Bear 1972; Barenblatt et al., 1984). In these cases, flow takes place only after the applied pressure gradient exceeds a certain minimum value, referred to as the threshold pressure gradient. The flow of oil in many heavy oil reservoirs does not follow Darcy's law, but it may be approximated by a Bingham fluid (Mirzadzandeh et al., 1971).

For groundwater flow in certain clayey soils, or in strongly argillized rocks, the existence of a threshold hydraulic gradient has also been observed. When the applied hydraulic gradient is below a certain minimum gradient, there is very little flow. This phenomenon was attributed by some authors to clay-water interactions (Bear, 1972; Mitchell, 1976).

The flow of foam in porous media is a focus of current research in many fields. Foam has been shown to be one of the most

promising fluids for mobility control in underground energy recovery or storage projects. On a macroscopic scale, flow behavior of foam in porous media is non-Newtonian. The "power-law" is generally used to correlate the apparent viscosities of foam with other flow properties for a given porous medium and a given surfactant (Patton et al. 1983; Hirasaki and Lawson, 1985). It has also been observed experimentally that foam will start to flow in a porous medium only after the applied pressure gradient exceeds a certain threshold value (Albrecht and Marsden, 1970; Witherspoon et al., 1989).

Drilling and hydraulic-fracturing fluids used in the oil industry are usually non-Newtonian liquids. Therefore, during well drilling or hydraulic-fracturing operations, the non-Newtonian drilling muds or hydraulic fluids will filtrate into permeable formations surrounding the wellbore, which may seriously damage the formation. The rheological behavior of drilling muds, cement slurries and hydraulic-fracturing fluids is often described by a Bingham plastic model (Robertson et al., 1976; Cloud and Clark, 1985). However, very little quantitative analysis has been reported on the formation response near the wellbore to non-Newtonian fluids.

At present, there is no standard approach in the petroleum engineering or groundwater literature for analyzing well test data for Bingham-type fluid production or injection. Interpretation of transient pressure responses of Bingham flow in porous media will be very important for heavy oil development, for groundwater flow evaluation in certain clayey formations, and for flow analysis of foam in porous media. The immiscible displacement of Non-Newtonian and Newtonian fluid occurs in many EOR processes, involving the injection of non-Newtonian fluids, such as polymer and foam solutions, or heavy oil production by waterflooding. However, very little research has been published on multiple phase flow of both non-Newtonian and Newtonian fluids through porous media. Even using numerical methods, very few studies have been performed to examine the physics of displacement (Gencer and Ikoku, 1984). Therefore, the mechanisms of immiscible displacement involving non-Newtonian fluids in porous media are still not well understood.

This paper presents a new methodology for analysis of the transient flow of Bingham fluids through porous media, including an integral analysis method for single phase flow and a Buckley-Leverett type analytical solution for two-phase immiscible displacement with Bingham non-Newtonian fluids. In order to apply the theory to field problems, a new well test analysis method has been developed, and its application is demonstrated by analyzing two simulated pressure drawdown and buildup tests of a Bingham fluid. The displacement of a Bingham fluid by a Newtonian fluid is shown to proceed with rather limited efficiency due to the presence of an ultimate (limited) displacement saturation, which is a characteristic of two-phase Bingham flow. Once the saturation in the two-phase flow system reaches the ultimate saturation, no further improvement of displacement efficiency can be obtained, regardless of how long the displacement operation continues under the same flow conditions.

We have also developed a numerical model for single- and multi-phase Bingham fluid flow through porous media, by suitably modifying a general-purpose multiphase reservoir simula-

tor. The model has been used to test our analytical solutions and the proposed well test analysis for Bingham fluids.

2. Bingham Fluid and Rheological Model

As a special kind of non-Newtonian fluids, Bingham fluids (or plastics) exhibit a finite yield stress at zero shear rate. The physical behavior of fluids with a yield stress is usually explained in terms of an internal structure in three dimensions which is capable of preventing movement for values of shear stress less than the yield value, τ_y . For shear stress τ larger than τ_y , the internal structure collapses completely, allowing shearing movement to occur. The characteristics of these fluids are defined by two constants: the yield stress τ_y which is the stress that must be exceeded for flow to begin, and the Bingham plastic coefficient μ_b . The rheological equation for a Bingham plastic is (Bird et al., 1960)

$$\tau = \tau_y + \mu_b \dot{\gamma} \quad (1)$$

where $\dot{\gamma}$ is the shear rate. The Bingham plastic concept has been found to closely approximate many real fluids existing in porous media, such as tarry and paraffin oils (Mirzadzandeh et al. 1971; Barenblatt et al., 1984), and drilling muds and fracturing fluids (Hughes and Brighton, 1967), which are suspensions of finely-divided solids in liquids.

For a phenomenological description of flow in porous media, some equivalent or apparent viscosities for non-Newtonian fluid flow are needed in Darcy's equation. Therefore, many experimental and theoretical investigations have been conducted to find rheological models, or correlations of apparent viscosities and flow properties for a given non-Newtonian fluid as well as a given porous material. For flow problems in porous media involving non-Newtonian Bingham fluids, the formulation of Darcy's law has been modified (Bear, 1972; Scheidegger, 1974; Barenblatt et al., 1984) to,

$$\bar{v} = - \frac{K}{\mu_b} \left[1 - \frac{G}{|\nabla P|} \right] \nabla P \quad (2a)$$

for $|\nabla P| > G$,

$$\bar{v} = 0 \quad (2b)$$

for $|\nabla P| \leq G$. Where K is formation permeability, P is pressure, and G is the minimum pressure gradient. The physical meaning of G can be elucidated by considering flow of a Bingham fluid through a capillary with radius R . The Bingham flow equation was solved by Buckingham (Skelland, 1967) to give the average flow velocity over the cross-section of the tube. By comparing this velocity with Darcy's law, we obtain

$$G = \frac{\tau_y}{3R/8} = \frac{\tau_y}{d} \quad (3)$$

where d is a characteristic pore size of a porous medium, $d = 3R/8$. Therefore, physically, the minimum pressure gradient G is the pressure gradient corresponding to the yield stress τ_y in a porous medium.

The two Bingham fluid parameters G and μ_b should be determined by laboratory experiments or well tests for a porous

media flow problem. The range of values for the minimum potential gradient G is quite large for different reservoirs. A reasonable value of G is on the order of 10^4 Pa/m for heavy oil (Mirzadzandeh et al., 1971), and it may exceed 3.0×10^5 Pa/m for groundwater flow in certain clayey soils (Bear, 1972).

3. Integral Analysis of Single-Phase Bingham Flow

The "integral method" has been widely used in the study of unsteady heat transfer problems (Ozisik, 1980). It is applied here to obtain an approximate analytical solution for Bingham fluid flow in porous media. The integral approach to heat conduction utilizes a simple parametric representation of the temperature profile, e.g. by means of a polynomial, which is based on physical concepts such as a time-dependent thermal penetration distance. An approximate solution of the heat transfer problem is then obtained from simple principles of heat flux continuity and energy conservation. This solution satisfies the governing partial differential equation only in an average, integral sense. However, it is encouraging to note that many integral solutions to heat transfer and fluid mechanics problems have an accuracy that is generally acceptable for engineering applications (Ozisik, 1980). When applied to fluid flow problems in porous media, the integral method consists of assuming a pressure profile in the pressure disturbance zone and determining the coefficients of the profile by making use of the integral mass balance equation (Wu, 1990).

In analogy to the heat conduction problem (Lardner and Pohle, 1961; Ozisik, 1980), we first assumed a pressure profile of the form

$$P(r, t) - P_i = [P_n(r)] \ln(r) \quad (r_w \leq r \leq r_w + \delta(t)) \quad (4)$$

where $P_n(r)$ is an n th-degree polynomial in r , and the time dependence is implicitly included in the coefficients of the polynomial, which is dependent on the pressure penetration distance $\delta(t)$ ($P_n(\delta) = 0$). However, we found that solutions in terms of profiles as given by Equation (4) are not accurate when compared to the Theis solution for the limiting case of a Newtonian fluid ($G = 0$), and always introduce 5-10 % errors. More accurate solutions were obtained for radial flow in a porous medium using pressure profiles of the form:

$$P(r, t) - P_i = \text{constant} \times \ln[P_n(r)] \quad (5)$$

3.1 Mathematical Formulation and Integral Solution

The problem considered here involves production of a Bingham fluid from a fully penetrating well in an infinite horizontal reservoir of constant thickness, and the formation is saturated only with the Bingham fluid. The basic assumptions are as follows:

- 1) isothermal, isotropic and homogeneous formation;
- 2) single phase horizontal flow without gravity effects;
- 3) Darcy's law, Equation (2), applies; and
- 4) constant fluid properties and formation permeability.

The governing flow equation can be derived by combining the modified Darcy's law with the continuity equation, and is

expressed in a radial coordinate system as

$$\frac{K}{r} \frac{\partial}{\partial r} \left[\frac{\rho(P)}{\mu_b} r \left[\frac{\partial P}{\partial r} - G \right] \right] = \frac{\partial}{\partial t} [\rho(P)\phi(P)] \quad (6)$$

The density, $\rho(P)$, of the Bingham fluid, and the porosity, $\phi(P)$, of the formation, are functions of pressure only.

The initial condition is

$$P(r, t=0) = P_i \quad (\text{Constant}) \quad (r \geq r_w) \quad (7)$$

At the inner boundary at the wellbore, $r = r_w$, the fluid is produced at a given mass production rate $Q_m(t)$; i.e.

$$\frac{2\pi r_w K h \rho(P_0)}{\mu_b} \left[\frac{\partial P}{\partial r} - G \right]_{r=r_w} = Q_m(t) \quad (8)$$

where $P_0 = P_0(t) = P(r_w, t)$, the wellbore pressure.

The integral solution for radial flow into a well under a specified mass production rate $Q_m(t)$ has been obtained, using the pressure profile of Equation (5) with an added inhomogeneous term, as (Wu, 1990)

$$P(r, t) = P_i + (r - r_w \eta) G - \frac{Q_m(t) \mu_b}{2\pi K h} \frac{1}{\rho(P_0)} \left[\frac{1 + 2\delta(t)/r_w}{2\delta(t)/r_w} \right] \times \ln \left[\frac{2r/r_w}{\eta} - \left[\frac{r/r_w}{\eta} \right]^2 \right] \quad (9)$$

where $\eta = 1 + \delta(t)/r_w$. The unknowns, P_0 , wellbore pressure, and $\delta(t)$, pressure penetration distance, are determined by simultaneously solving Equation (9) and the following integral equation,

$$\int_{r_w}^{r_w + \delta(t)} 2\pi h r \rho(P) \phi(P) dr = - \int_0^t Q_m(t) dt + \pi h \rho_i \phi_i [(r_w + \delta(t))^2 - r_w^2] \quad (10)$$

where $\rho_i = \rho(P_i)$, and $\phi_i = \phi(P_i)$. Equation (10) is simply a mass balance equation in the pressure disturbance region.

For slightly compressible flow, we obtain the following explicit expression of the integral mass balance equation

$$\int_0^t Q_m(t) dt + \rho_i \phi_i C_{tr_w}^2 \left[2\pi h r_w G \left[-\frac{1}{6} \eta^3 + \frac{1}{2} \eta - \frac{1}{3} \right] + \frac{Q_m(t) \mu_b}{K \rho(P_0)} \left[\frac{1 + 2\delta(t)/r_w}{2\delta(t)/r_w} \right] \left[-\frac{3}{2} \eta^2 + \eta + \frac{1}{2} + 2\eta \ln(\eta) - \frac{1}{2} [1 - 4\eta^2] \ln \left[\frac{2\eta - 1}{\eta^2} \right] \right] \right] = 0 \quad (11)$$

3.2 Verification of Integral Solutions

The solution from the integral method is approximate and needs to be checked by comparison with an exact solution or

with numerical results. In this section, the accuracy of the integral solution obtained in Section 3.1 is examined and confirmed by comparison with an exact solution in a special case and with numerical calculations.

a) Comparison with Exact Solution

For the special case of minimum pressure gradient $G = 0$, a Bingham fluid becomes Newtonian. Then, the Theis solution can be used to check the integral solution, given by Equations (9) and (11). A comparison of the exact Theis solution and the integral solution using parameters as given in Table 1, with $G = 0$, is presented in Figures 1 and 2. Essentially, no differences can be observed between the wellbore pressures calculated from the two solutions in Figure 1. There are only minor errors near the pressure penetration front of the pressure profile after 1,000 seconds of injection (Figure 2). Many additional comparisons using different fluid and formation properties have been performed between the integral and Theis solutions, and excellent agreement has been obtained in all cases.

b) Comparison with Numerical Solution

For the radial flow problem of Bingham fluid production with $G > 0$, the results from the integral solution have been examined by comparison with numerical simulations. The wellbore flowing pressures calculated from the integral and numerical solutions are shown in Figure 3. It is interesting to note that the agreement between the approximate integral and numerical results is excellent for the entire transient flow period. The pressure distribution in the formation after 1,000 seconds, as shown in Figure 4, also matches the numerical predictions extremely well.

By comparison of the integral solutions with both the exact Theis solution and the numerical simulation, it is concluded that the pressure profile, Equation (5), can accurately represent radial flow of both Newtonian and Bingham fluids.

3.3 Effects of Minimum Pressure Gradient

For the problem specified in Table 1, we have utilized the integral solution to examine flow behavior for a range of rheological parameters. The pressure drawdown at the wellbore for constant mass production rate is shown in Figure 5. The flow resistance increases with an increase in the minimum pressure gradient G in a reservoir. Therefore, in order to maintain the same production rate, the wellbore pressure decreases more rapidly with increasing G , as indicated in Figure 5. The pressure profiles after continuous production of 10 hours at different values of G are shown in Figure 6. As the minimum pressure gradient increases, the pressure drops penetrate less deeply into the formation because of larger flow resistance.

3.4 Well Testing Analysis of Bingham Fluid Flow

An analysis method for transient pressure tests during Bingham fluid production or injection into a well can be developed,

based on the integral and numerical solutions of this work. The most important parameters for Bingham fluid flow through porous media are the two characteristic rheological parameters, the minimum pressure gradient, G , and the coefficient, μ_b . It is always possible to obtain these parameters by trial and error, using the integral and numerical solutions to match the observed pressure data. However, the following approach is more accurate and convenient to use, and is recommended for field applications.

Let us consider the pressure buildup behavior in an infinite horizontal formation with a production well. After some period of production, the well is shut in. The pressure in the system will build up until a new equilibrium is achieved at a long enough shut-in period, theoretically infinite time. The pressure gradient everywhere in the pressure penetration zone is expected to be equal to the minimum pressure gradient. This is confirmed by a numerical study of the pressure buildup, as shown in Figure 7, after $t_p = 1,000$ seconds of Bingham fluid production from a well. If the cumulative mass production rate Q_c before the well is shut in is known, the minimum pressure gradient of the system can be calculated from the observed stabilized wellbore pressure P_w (Wu, 1990) by

$$G = \frac{1}{2Q_c} \left[\pi h r_w \rho_i \phi_i C_i (\Delta P)^2 + \left[(\pi h r_w \rho_i \phi_i C_i (\Delta P)^2)^2 + 4\pi h \rho_i \phi_i C_i (\Delta P)^3 / 3 \right]^{1/2} \right] \quad (12)$$

where $\Delta P = P_i - P_w$. It is interesting to note that the minimum pressure gradient determined by the pressure buildup method, as given in Equation (12), is independent of the flow properties, such as permeability K , and the coefficient μ_b , since it pertains to equilibrium in the system.

To illustrate the procedure of calculating the value of G , a test example was created by numerical simulation. A Bingham fluid is produced at a mass rate $Q_m = 0.1$ kg/s until the production time $t_p = 1,000$ seconds, and then the well is shut in. The stable wellbore pressure is found to be $P_w = .97474 \times 10^7$ Pa, at a long shut-in time. Thus, the minimum pressure gradient can be calculated by Equation (12)

$$G = \frac{1}{200} \left[1.1737 \times 10^5 + \left[1.377 \times 10^8 + 3.953 \times 10^{12} \right]^{1/2} \right] \\ = 10,000.14 \text{ (Pa/m)} \quad (13)$$

This is very accurate compared with the input value, $G = 10,000$ Pa/m, in the numerical calculation. The pressure penetration distance at equilibrium is,

$$\delta(t) = \frac{\Delta P}{G} = \frac{2.526 \times 10^5}{10,000.14} = 25.26 \text{ (m)} \quad (14)$$

The pressure distribution after a long shut-in time calculated from the mass balance is also shown in Figure 7. The analytical and numerical results are essentially identical to each other.

The apparent mobility, (K/μ_b) , is a flow property of the system, and may be determined by transient flow tests, when the minimum pressure gradient, G , is not very large. Figure 5 shows that semi-log straight lines occur in the pressure drawdown curves during the early transient period; they are almost parallel to the straight line from the Theis solution ($G = 0$). Therefore, if the semi-log straight line is developed during the

early flow time in the transient pressure drawdown, the conventional analysis technique (Earlougher, 1977; Matthews and Russell, 1967) can be used to estimate the value of (K/μ_b) for a Bingham fluid. For example, the slope m of the semi-log straight line part of the curve $G = 100$ Pa/m, in Figure 5, is measured as 9.23574×10^4 Pa/log₁₀-cycle. Then, K/μ_b can be estimated as

$$\frac{K}{\mu_b} = \frac{2.303 \times 0.5 / 1000.0}{4 \times 3.1415926 \times 1.0 \times 9.23574 \times 10^4} = 9.92 \times 10^{-10} \text{ (m}^2/\text{Pa}\cdot\text{s)} \quad (15)$$

In the simulated test, the actual input is

$$\frac{K}{\mu_b} = \frac{0.9869 \times 10^{-12}}{1.0 \times 10^{-3}} = 9.87 \times 10^{-10} \text{ (m}^2/\text{Pa}\cdot\text{s)} \quad (16)$$

so that the relative error is only 0.5 %.

For a large value of the minimum pressure gradient G , there hardly exist semi-log straight lines in the pressure drawdowns. However, the pressure buildup curves, as shown in Figures 8, do result in a long straight line even for a large minimum pressure gradient of $G = 10,000$ Pa/m. This pressure buildup test is conducted by the numerical code. The top curve in Figure 8 is the prediction from the integral solution, based on the superposition principle. As expected, the superposition technique cannot be used for this non-linear problem. The slope of the semi-log straight line of Figure 8 is measured as $m = 9.169043 \times 10^4$ log₁₀-cycle. Then, we have

$$\frac{K}{\mu_b} = \frac{2.303 \times 0.1 / 975.9}{4 \times 3.1415926 \times 1.0 \times 9.169043 \times 10^4} = 2.05 \times 10^{-10} \text{ (m}^2/\text{Pa}\cdot\text{s)} \quad (17)$$

This value differs only by 3.8 % from the input value, $K/\mu_b = 1.97 \times 10^{-10}$ m²/Pa·s.

If no straight lines are developed in either pressure drawdown or pressure buildup curves, then the apparent mobility can be obtained by using the integral solution to match the observed transient pressure data. The minimum pressure gradient G should always be calculated first from the mass balance, Equation (12), which is always applicable. The only remaining unknown is then the apparent mobility (K/μ_b) , which can be easily determined by trial and error using the integral solution.

4. Immiscible Displacement of a Bingham Non-Newtonian Fluid by a Newtonian Fluid

In an effort to obtain some insight into the physics behind two-phase immiscible displacement with non-Newtonian fluids, we have developed a Buckley-Leverett type analytical solution for one-dimensional flow in porous media (Wu, Pruess and Witherspoon, 1989). Here, this analytical solution is used to study the displacement of a Bingham-type non-Newtonian fluid by a Newtonian fluid. One possible application of this study is the production of heavy oil by waterflooding. Note that because of the one-dimensional approximation in our analysis we cannot address issues of viscous or gravitational instabilities.

4.1 Analytical Solution for Bingham Fluid Displacement

The analytical solution obtained for immiscible non-Newtonian fluid displacement (Wu et al., 1989) is in the same form as the Buckley-Leverett frontal advance equation (1942). The crucial difference is in the fractional flow function which now depends not only on relative permeability data, but also, through apparent or effective viscosities, on the rheological properties of the non-Newtonian fluid. This feature introduces a strong rate-dependence into the displacement process, as will be seen below. The fractional flow function of the displacing Newtonian fluid is defined as the ratio of flow rate of the Newtonian fluid and the total rate, and is given by (Willhite, 1986):

$$f_{ne} = \frac{1}{1 + \left[\frac{k_{rn}(S_{ne})}{k_{me}(S_{ne})} \right] \left[\frac{\mu_{ne}}{\mu_{nn}} \right]} + \frac{A K k_{rn}(S_{ne})}{\mu_{nn} q(t)} (\rho_{nn} - \rho_{ne}) g \sin \alpha \quad (18)$$

$$1 + \left[\frac{k_{rn}(S_{ne})}{k_{me}(S_{ne})} \right] \left[\frac{\mu_{ne}}{\mu_{nn}} \right]$$

where S_{ne} is saturation of the displacing Newtonian fluid, k_{me} and k_{rn} are relative permeabilities to Newtonian and non-Newtonian phases, respectively, μ_{ne} is the viscosity of the Newtonian fluid, and μ_{nn} is the apparent viscosity of the non-Newtonian fluid, which is a function of saturation and flow potential gradient:

$$\mu_{nn} = \mu_{nn}(\nabla \Phi, S_{nn}) \quad (19)$$

Introducing coordinates such that flow takes place in the x direction, the potential gradient component in the x direction is

$$\frac{\partial \Phi}{\partial x} = \frac{\partial P}{\partial x} + \rho_{nn} g \sin \alpha \quad (20)$$

where α is the angle between the horizontal plane and the flow direction.

Equations (18) and (19) indicate that the fractional flow f_{ne} of the displacing Newtonian phase is generally a function of both saturation and potential gradient. However, under the usual simplifications made in the Buckley-Leverett problem (incompressible, one-dimensional linear flow, uniform fluid and formation properties), the potential gradient is uniquely related to saturation as follows (Wu et al., 1989)

$$q(t) + A K \left[\frac{k_{me}(S_{nn})}{\mu_{ne}} + \frac{k_{rn}(S_{nn})}{\mu_{nn}(\partial \Phi / \partial x, S_{nn})} \right] \frac{\partial P}{\partial x} + K \left[\frac{\rho_{ne} k_{me}(S_{nn})}{\mu_{ne}} + \frac{\rho_{nn} k_{rn}(S_{nn})}{\mu_{nn}(\partial \Phi / \partial x, S_{nn})} \right] g \sin \alpha = 0 \quad (21)$$

Therefore, the fractional flow function in Equation (18) ends up being a function of saturation only, and the Welge (1952) graphic method can be applied for evaluation of non-Newtonian fluid displacement (Wu et al., 1989). The rheological model for the apparent viscosity of a Bingham plastic fluid can be obtained from Equation (2),

$$\mu_{mn} = \frac{\mu_b}{1 - \frac{G}{|\partial\Phi/\partial x|}} \quad (22a)$$

for $|\partial\Phi/\partial x| > G$, and

$$\mu_{mn} = \infty \quad (22b)$$

for $|\partial\Phi/\partial x| \leq G$. For a particular saturation S_{ne} of the Newtonian phase, the corresponding flow potential gradient for the non-Newtonian phase can be derived by introducing Equation (22a) into Equation (21) as follows:

$$-\left(\frac{\partial\Phi}{\partial x}\right)_{S_{ne}} = -\rho_{mn} g \sin\alpha + \frac{\frac{q}{AK} + \frac{k_{me}(S_{ne})}{\mu_{ne}} \rho_{ne} g \sin\alpha + \frac{k_{mn}(S_{ne})}{\mu_b} [\rho_{mn} g \sin\alpha + G]}{\frac{k_{me}(S_{ne})}{\mu_{ne}} + \frac{k_{mn}(S_{ne})}{\mu_b}} \quad (23)$$

The apparent viscosity for the Bingham fluid is determined by using Equation (23) in (22), and then the fractional flow curve is calculated from Equation (18).

4.2 Displacement of a Bingham Non-Newtonian Fluid by a Newtonian Fluid

Initially, the system is assumed to be saturated with only a Bingham fluid, and a Newtonian fluid is injected at a constant volumetric rate at the inlet, $x = 0$, starting from $t = 0$. The relative permeabilities are given as functions of saturation of the displacing Newtonian fluid in Figure 9, calculated from the analytical correlation by Willhite (1986). The fluid and rock properties are summarized in Table 2. Some fundamental behavior of Bingham type non-Newtonian fluid displacement will now be discussed.

a) Effects of Non-Newtonian Rheological Properties

A basic feature of the displacement process of a Bingham fluid in porous media is the existence of an ultimate or maximum displacement saturation, S_{max} , for the displacing Newtonian phase (see Figures 10 and 11). The maximum displacement saturation occurs at the point of the fractional flow curve where $f_{ne} = 1.0$. For this particular displacement system, initially saturated only with the Bingham fluid, the displacing saturation cannot exceed the maximum value S_{max} . The resulting saturation distributions are given in Figure 11 for different minimum pressure gradients G . It is obvious that the sweep efficiency decreases rapidly as G increases. In contrast, for Newtonian displacement, the ultimate saturation of the displacing fluid is equal to the total mobile saturation of the displaced fluid, as shown by the curve for $G = 0$ in Figure 11.

Physically, the phenomenon of ultimate displacement saturation occurs as the flow potential gradient approaches the minimum threshold pressure gradient G , at which the apparent viscosity is infinite. Then the only flowing phase is the displacing Newtonian fluid. Consequently, once the maximum saturation has been reached for a flow system, no improvement of

sweep efficiency can be obtained no matter how long the displacement process continues, as shown in Figure 11. The flow condition in reservoirs is more complicated than in this linear semi-infinite system. Since oil wells are usually drilled according to certain patterns, there always exist some regions with low potential gradients between production and injection wells. The presence of the ultimate displacement saturation for a Bingham fluid indicates that no oil can be driven out of these regions. Therefore, the ultimate displacement saturation phenomenon will contribute to the low oil recovery observed in heavy oil reservoirs developed by water-flooding, in addition to effects from the high oil viscosity.

The effects of the other rheological parameter, the Bingham plastic coefficient μ_b , are shown in Figure 12. It is interesting to note that the ultimate displacement saturations change little with μ_b . However, the average saturations in the swept zones are quite different for different values of μ_b . The ultimate displacement saturation is essentially determined by the minimum pressure gradient G . Changes in μ_b have little effect on the ultimate displacement saturation since the flow potential gradient in Equation (23), hardly varies with μ_b as $\partial P/\partial x \rightarrow G$.

b) Comparison with Numerical Simulation

Numerical simulation of two-phase immiscible displacement of a Bingham fluid is difficult because of discontinuities in saturation profiles and pressure gradients. There is the familiar Buckley-Leverett saturation shock front, and in addition there is a discontinuity in saturation (and pressure) derivatives at the leading edge where the ultimate displacement saturation has been reached (see Figure 11). The latter is associated with the extremely strong nonlinearity of apparent Bingham fluid viscosities becoming infinite. A finite-difference simulation of this process is subject to numerical dispersion effects.

A comparison of the saturation profiles from the numerical and analytical calculations after 10 hours of Newtonian fluid injection is given in Figure 13. Overall, the numerical results are in good agreement with the analytical solution. It is particularly significant that the ultimate displacement saturation is extremely well predicted. Only near the discontinuities in saturation and saturation gradient does the numerical solution introduce certain errors because of numerical dispersion. The numerical difficulties are largely due to the (unphysical) assumption of incompressible fluids and formation, and neglect of capillary pressures, which are essential to the Buckley-Leverett type solution. The finite-difference simulation requires a finite, albeit small compressibility.

c) Effects of Injection Rate

In this problem, a Bingham fluid in a horizontal porous medium is displaced by water. If water injection rate at the inlet is increased, the pressure gradient in the system will increase, and the apparent viscosity for the displaced Bingham fluid will be reduced. Therefore, a better sweep efficiency will result. Figure 14 presents the saturation profiles after injection of 10 hours with the different rates. It is interesting to note that both the sweep efficiency and the ultimate displacement saturation can be greatly increased by increasing the injection rate.

d) Effects of Gravity

The effects of gravity on Bingham fluid displacement by a Newtonian fluid can be examined by considering the following example. A heavier Newtonian fluid with density $\rho_{ne} = 1,000 \text{ kg/m}^3$ is used to displace a Bingham fluid with density $\rho_{nn} = 850 \text{ kg/m}^3$. The flow directions are upwards ($\alpha = \pi/2$), horizontal ($\alpha = 0$), and downwards ($\alpha = -\pi/2$). The saturation distributions after 10 hours of displacement are shown in Figure 15. The difference in density of the two fluids is small, so the influence of gravity on displacement efficiency near the front is not very significant. However, gravity does change the ultimate displacement saturation. The best displacement performance is obtained by upwards flow. Since gravity resists the upwards flow of the heavier displacing phase, the flow potential gradient must be larger in order to maintain the same flow rate. Consequently, the apparent viscosity of the Bingham fluid is decreased for upwards flow resulting in the better sweep efficiency.

5. Conclusions

An approximate integral solution has been obtained for the problem of Bingham flow through porous media. Its accuracy has been confirmed by comparison with exact and numerical solutions. Our analytical and numerical studies show that the transient flow behavior of slightly compressible Bingham fluids is essentially controlled by the non-Newtonian properties, namely, the minimum pressure gradient G , and the Bingham plastic coefficient μ_b . Therefore, transient pressure data can provide important information related to the non-Newtonian fluid and formation properties. A well test analysis technique developed in this study uses flow test data to estimate non-Newtonian flow properties.

The integral method with a new pressure profile developed in this work is applicable to more general radial flow problems in porous media. It is especially useful when the flow equation is nonlinear and other analytical approaches cannot apply.

The fundamental feature of immiscible displacement involving a Bingham plastic fluid is that there exists an ultimate displacement saturation, which is essentially determined by the minimum pressure gradient G . This saturation can be considerable larger than residual saturations from relative permeability effects. Once the saturation approaches the ultimate saturation in the formation, no further displacement can be obtained regardless of how long the displacement lasts for a given operating condition. A simple way to gain a better sweep efficiency is to increase injection rates, thereby reducing the apparent viscosity of the displaced Bingham fluid. A better displacement can also be obtained by using gravity to increase the flow potential gradient in the flow direction for a given flow rate.

Nomenclature

A	Cross-sectional area, m^2
C_f	Fluid compressibility, Pa^{-1}

C_f	Formation compressibility, Pa^{-1}
C_t	Total compressibility, Pa^{-1}
f_{ne}	Fractional flow of Newtonian phase
f_{nn}	Fractional flow of non-Newtonian phase
g	Magnitude of the gravitational acceleration, m/s^2
G	Minimum pressure gradient, Pa/m
h	Formation thickness, m
K	Absolute permeability, m^2
k_{rne}	Relative permeability to Newtonian phase
k_{rnn}	Relative permeability to non-Newtonian phase
m	Slope of semi-log curves, $\text{Pa}/\log\text{-cycle}$
NK	Number of fluid components
NPH	Number of fluid phases
P	Pressure, Pa
P_i	Initial formation pressure, Pa
$P_n(r)$	n th-degree polynomial in r
P_w	Wellbore flowing pressure, Pa
∇P	Pressure gradient, Pa/m
$q(t)$	Volumetric injection rate, m^3/s
Q	Volumetric production/injection rate, m^3/s
Q_c	Cumulative mass production, kg
$Q_m(t)$	Mass injection/production rate, kg/s
r	Radial distance, coordinate, m
R	Radius of a tube, m
r_w	Wellbore radius, m
S	Saturation
S_{max}	Ultimate displacement saturation
S_{ne}	Newtonian phase saturation
S_{nn}	Non-Newtonian phase saturation
S_{nnir}	Irreducible Non-Newtonian phase saturation
S_{ne}	Average Newtonian phase saturation
t	Time, s
u	Darcy velocity, m/s
\vec{u}	Darcy velocity vector, m/s
x	Distance from inlet, coordinate, m

Greek Symbols

α	Angle between flow direction and horizontal plane
γ	Shear Rate, s^{-1}
$\delta(t)$	Pressure penetration distance, m
μ_b	Bingham plastic coefficient, $\text{Pa}\cdot\text{s}$
μ_{ne}	Newtonian viscosity, $\text{Pa}\cdot\text{s}$
μ_{nn}	Non-Newtonian apparent viscosity, $\text{Pa}\cdot\text{s}$
η	$\eta = 1 + \delta(t)/r_w$
ρ_i	Initial fluid density, kg/m^3
ρ_{ne}	Density of Newtonian fluid, kg/m^3
ρ_{nn}	Density of non-Newtonian fluid, kg/m^3
τ	Shear stress, Pa
τ_y	Yield stress, Pa
ϕ	Porosity
Φ	Flow potential, Pa
ϕ_i	Initial formation porosity
$\nabla\Phi$	Flow potential gradient, Pa/m
$\nabla\Phi_e$	Effective flow potential gradient, Pa/m

Subscripts

b	Bingham fluid
e	Equivalent

i	Initial
m	Mass
n	nth degree
ne	Newtonian fluid
nn	Non-Newtonian fluid
rne	Relative to Newtonian fluid
rnn	Relative to non-Newtonian fluid
t	Total
w	Wellbore
y	Yield

Acknowledgment

For a critical review of the manuscript the authors are grateful to R. W. Zimmerman and M. Ripperda. This work was supported by the Office of Basic Sciences, U. S. Department of Energy, under Contract No. DE-AC03-76SF00098.

References

- Albrecht, R. A. and Marsden, S. S. (1970) : "Foams as Blocking Agents in Porous Media," *Soc. Pet. Eng. J.*, 51.
- Barenblatt, G. E., Entov, B. M. and Rizhik, B. M. (1984) : *Flow of Liquids and Gases in Natural Formations*, Nedra, Moscow.
- Bear, J. (1972) : *Dynamics of Fluids in Porous Media*, American Elsevier, New York.
- Bird, R. B., Stewart, W. E. and Lightfoot, E. N. (1960) : *Transport Phenomena*, Wiley, New York.
- Buckley, S. E. and Leverett, M. C. (1942) : "Mechanism of Fluid Displacement in Sands," *Trans.*, AIME 146, 107-116.
- Cloud, J. E. and Clark, P. E. (1985) : "Alternatives to the Power-Law Fluid Models for Crosslinked Fluids," *Soc. Pet. Eng. J.*, 609-618.
- Duff, I. S. (1977) : "MA28 - A Set of Fortran Subroutine for Sparse Unsymmetric Linear Equations," AERE Harwell Report R 8730.
- Earlougher, R. C. Jr. (1977) : *Advances in Well Test Analysis*, SPE Monograph Series, Vol. 5.
- Gencer, C. S. and Ikoku, C.U. (1984) : "Well Test Analysis for Two-Phase flow of Non-Newtonian Power-law and Newtonian Fluids," *ASME Journal of Energy Resources Technology*, 295-304.
- Gogarty, W. B. (1967) : "Rheological Properties of Pseudo Plastic Fluids in Porous Media," *Soc. Pet. Eng. J.*, 149-159.
- Hirasaki, G. J. and Lawson, J. B. (1985) : "Mechanisms of Foam Flow in Porous Media: Apparent Viscosity in Smooth Capillaries," *Soc. Pet. Eng. J.*, 176-190.
- Hughes, W. F. and Brighton, J. A. (1967) : *Theory and Problems of Fluid Dynamics*, Schaum's Outline Series, McGraw-Hill Book Co., 230-241.
- Ikoku, C. U. and Ramey, H. J. Jr. (1979) : "Transient Flow of Non-Newtonian Power-Law Fluids in Porous Media," *Soc. Pet. Eng. J.*, 164-174.

- Lardner, T. J. and Pohle, F. V. (1961) : "Application of the Heat Balance integral to Problems of Cylindrical Geometry," *J. Appl. Mech., Trans. ASME*, 310-312.
- Mathews, C. S. and Russell, D. G. (1967) : *Pressure Buildup and Flow Tests in wells*, Monograph Series, Society of Petroleum engineers AIME, Dallas.
- Mirzadzanzade, A. KH., Amirov, A. D., Akhmedov, Z. M., Barenblatt, G. I., Gurbanov, R. S., Entov, V. M., and Zaitsev, YU. V. (1971) : "On the Special Features of Oil and Gas Field Development Due to Effects of Initial Pressure Gradient," *Preprints of Proceedings of 8th World Petroleum Congress, Special Papers*. Elsevier London.
- Mitchell, J. K. (1976) : *Fundamentals of Soil Behavior*, John Wiley & Sons, Inc., New York.
- Narasimhan, N. T. and Witherspoon, P. A. (1976) : "An Integrated Finite Difference Method for Analyzing Fluid Flow in Porous Media," *Water Resources Research*, Vol.12, No.1, 57-64.
- Odeh, A. S. and Yang, H. T. (1979) : "Flow of Non-Newtonian Power-Law Fluids through Porous Media," *Soc. Pet. Eng. J.*, 155-163.
- Ozisik, M. N. (1980) : *Heat Conduction*, John Wiley and Sons.
- Patton, J. T., Holbrook, S. T. and Hsu, W. (1983) : "Rheology of Mobility-Control Foams," *Soc. Pet. Eng. J.*, 456-460.
- Pruess, K. (1988) : "SHAFT, MULKOM, TOUGH: a Set of Numerical Simulators for Multiphase Fluid and Heat Flow," Report LBL-24430, Earth Sciences Division, Lawrence Berkeley Laboratory, Berkeley, CA.
- Pruess, K. (1983) : "Development of the General Purpose Simulator MULKOM," *Annual Report*, Earth Sciences Division, Lawrence Berkeley Laboratory, Berkeley CA.
- Pruess, K. and Wu, Y.-S. (1988) : "On PVT-Data, Well Treatment, and Preparation of Input Data for an Isothermal Gas-Water-Foam Version of MULKOM," Report LBL-25783, UC-403, Earth Sciences Division, Lawrence Berkeley Laboratory, Berkeley, CA.
- Robertson, R. E. and Stiff, H. A. Jr. (1976) : "An Improved Mathematical Model for relating Shear Stress to Shear Rate in Drilling Fluids and Cement Slurries," *Soc. Pet. Eng. J.*, 31-36.
- Savins, J. G. (1969) : "Non-Newtonian Flow through Porous Media," *Ind. Eng. Chem.*, 61, 18-47.
- Scheidegger, A. E. (1974) : *The Physics of Flow through Porous Media*, University of Toronto Press.
- Skelland, A. H. P. (1967) : *Non-Newtonian Flow and Heat Transfer*, John Wiley & Sons, Inc. New York, London, and Sydney.
- van Poolen, H. K. and Jargon, J. R. (1969) : "Steady-State and Unsteady-State Flow of Non-Newtonian Fluids through Porous Media," *Soc. Pet. Eng. J., Trans.*, AIME 246, 80-88.
- Welge, H. J. (1952) : "A Simplified Method for computing Oil Recovery by Gas or Water Drive," *Trans.*, AIME 3, 108.
- Willhite, G. P. (1986) : *Waterflooding*, SPE Textbook, Series, Society of Petroleum Engineers, Richardson, TX.
- Witherspoon, P. A., Benson, S., Persoff, P., Pruess, K., Radke, C. J. and Y. -S. Wu (1989) : "Feasibility Analysis and

Development of Foam Protected Underground Natural Gas Storage Facilities," Final Report, Earth Sciences Division, Lawrence Berkeley Laboratory, CA.

Wu, Y. -S. (1990) : "Theoretical Studies of Non-Newtonian and Newtonian Fluid Flow through Porous Media," Ph. D. Thesis (in Preparation), Earth Sciences Division, Lawrence Berkeley Laboratory, University of California, Berkeley, CA.

Wu, Y. -S., Pruess, K. and Witherspoon, P. A. (1989) : "Displacement of a Newtonian Fluid by a Non-Newtonian Fluid in a Porous Medium," Submitted for publication to "Transport in Porous Media", Report LBL-27412, Earth Sciences Division, Lawrence Berkeley Laboratory, CA.

Appendix A. Numerical Model

The numerical simulations reported in this paper were performed with a modified and enhanced version of the general-purpose multiphase simulator MULKOM (Pruess, 1983; 1988). MULKOM uses an "integral finite difference" method (Narasimhan and Witherspoon, 1976) to solve discretized mass balance equations for NK fluid components distributed among NPH phases. Time is discretized as a first order finite difference, and all flow terms are formulated fully implicitly for numerical robustness and stability. Discretization results in a set of nonlinear algebraic equations which are solved by means of Newton-Raphson iteration. The linear algebra is performed with a sparse version of Gaussian elimination (Duff, 1977). A more detailed description of the code is available in laboratory reports (Pruess, 1988; Pruess and Wu, 1988).

The apparent viscosity functions for non-Newtonian fluids in porous media depend on the pore velocity, or the potential gradient, in a complex way. The rheological correlations for various non-Newtonian fluids are quite different. Therefore, it is impossible to develop a general numerical scheme which is universally applicable to all non-Newtonian fluids. Instead, a special treatment for a particular fluid of interest has to be worked out.

The flow of Bingham fluids is treated in the code by introducing an effective potential gradient $\nabla\Phi_e$, whose scalar component in the flow direction, assumed to be the x direction, is defined as

$$\left[\nabla\Phi_e \right]_x = \begin{cases} (\nabla\Phi)_x - G & (\nabla\Phi)_x > G \\ (\nabla\Phi)_x + G & (\nabla\Phi)_x < -G \\ 0 & -G \leq (\nabla\Phi)_x \leq G \end{cases} \quad (A.1)$$

Darcy's law for a Bingham fluid is used in the code in the form

$$\vec{u} = - \frac{K}{\mu_b} \nabla\Phi_e \quad (A.2)$$

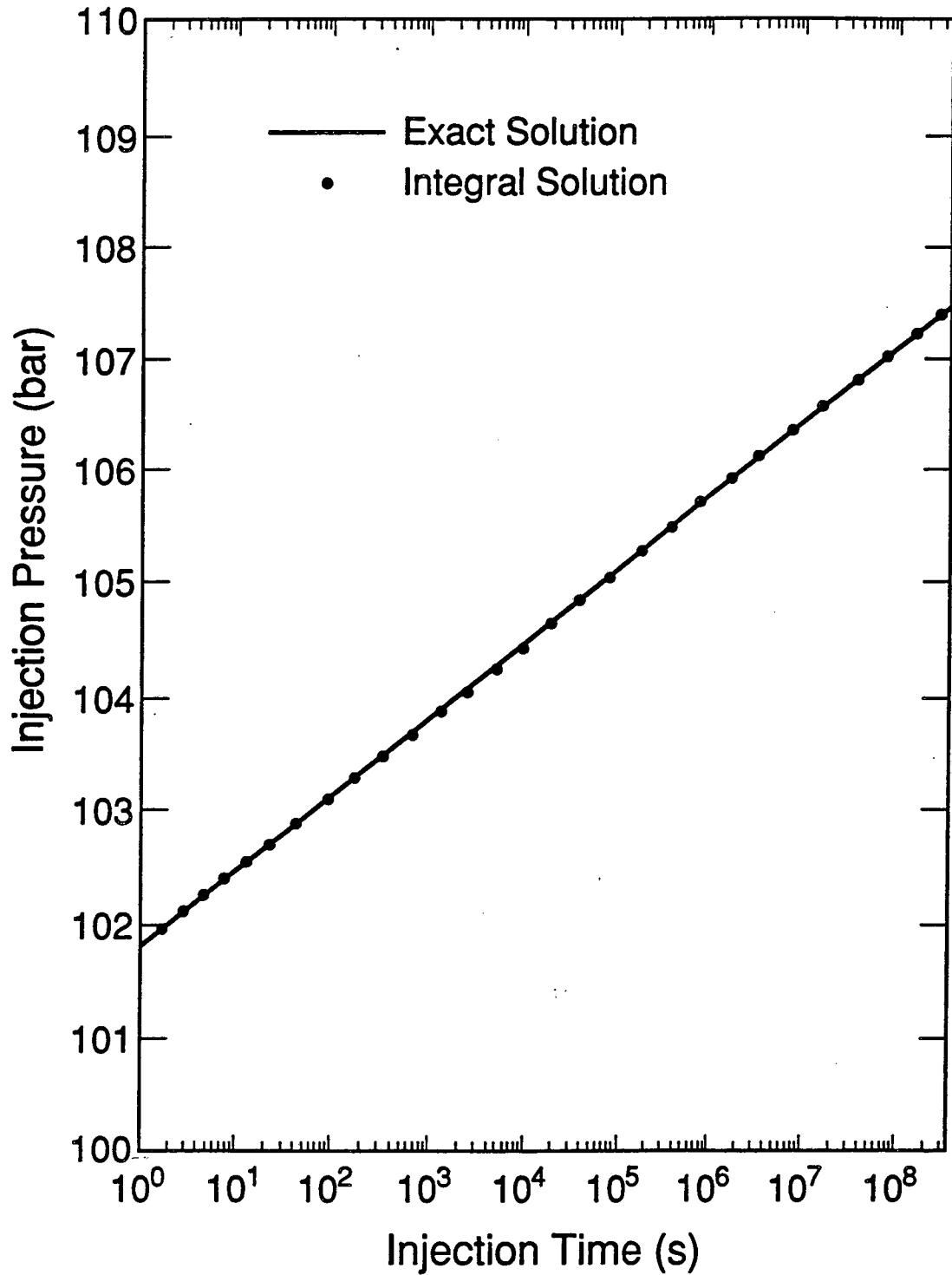
This treatment is much more efficient for simulation of Bingham fluid flow in porous media than the direct use of a highly nonlinear apparent viscosity as in Equation (22a).

Table 1
Parameters for Single Phase Bingham Fluid Flow

Initial pressure	$P_i=10^7\text{Pa}$
Initial Porosity	$\phi_i=0.20$
Initial Fluid Density	$\rho_i=975.9\text{kg/m}^3$
Formation Thickness	$h=1\text{m}$
Fluid Viscosity	$\mu_{ne}=.35132\times 10^{-3}\text{Pa}\cdot\text{s}$
Bingham Coefficient	$\mu_b=5\times 10^{-3}\text{Pa}\cdot\text{s}$
Fluid Compressibility	$C_f=4.557\times 10^{-10}\text{Pa}^{-1}$
Rock Compressibility	$C_r=5\times 10^{-9}\text{Pa}^{-1}$
Mass Injection Rate	$Q_m=1\text{kg/s}$
Permeability	$K=9.869\times 10^{-13}\text{m}^2$
Wellbore Radius	$r_w=0.1\text{m}$
Minimum Pressure Gradient	$G=0,10^2,10^3,10^4\text{Pa/m}$

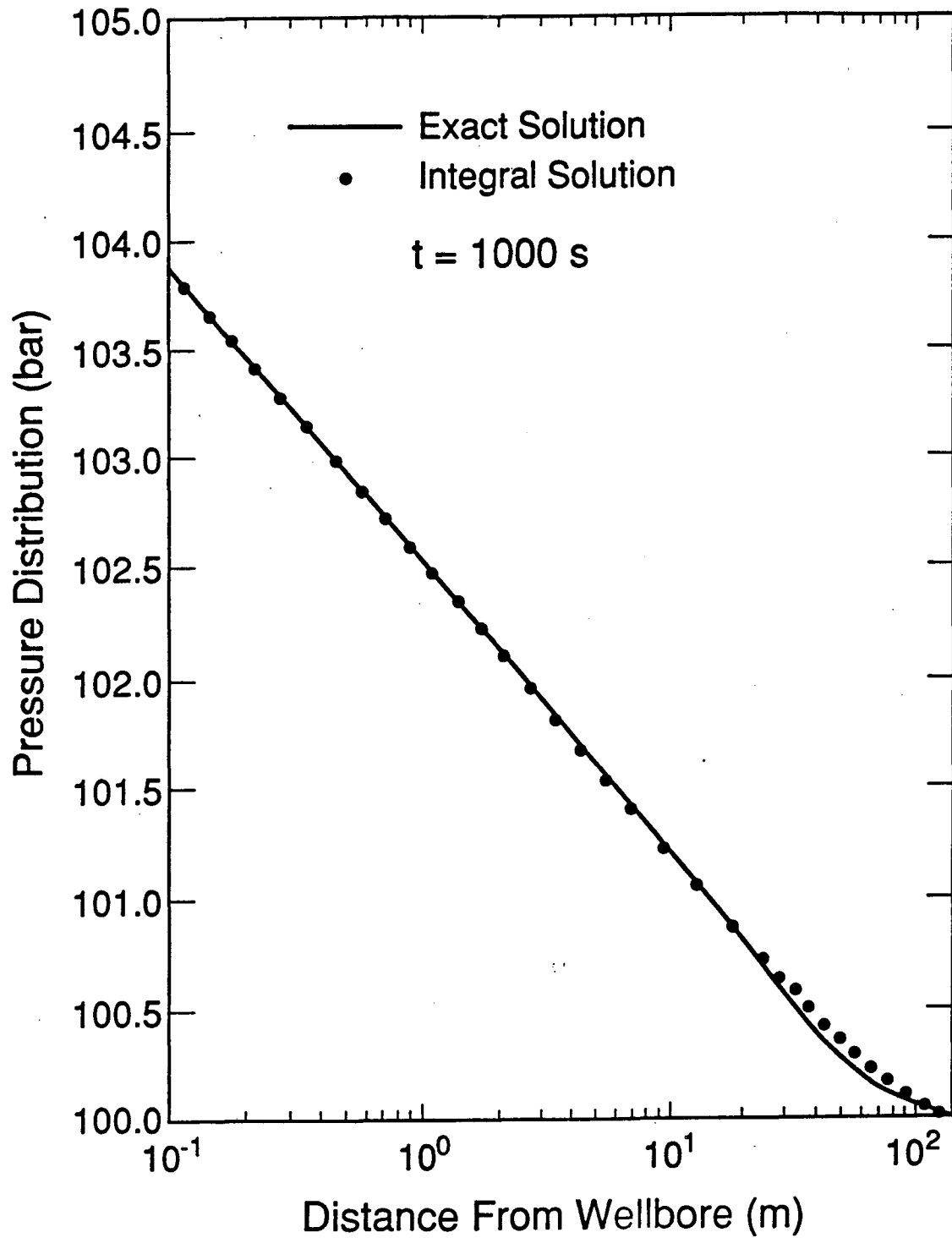
Table 2
Parameters for Linear Bingham Fluid Displacement

Porosity	$\phi=0.20$
Permeability	K=1 darcy
Cross-Sectional Area	1 m ²
Injection Rate	q=1.0×10 ⁻⁶ m ³ /s
Injection Time	T=10 hrs
Displacing Newtonian Viscosity	$\mu_{nc}=1$ cp
Irreducible Saturation	$S_{nir}=0.20$
Bingham Plastic Coefficient	$\mu_b=4.0$ cp
Minimum Pressure Gradient	G= 10,000 Pa/m



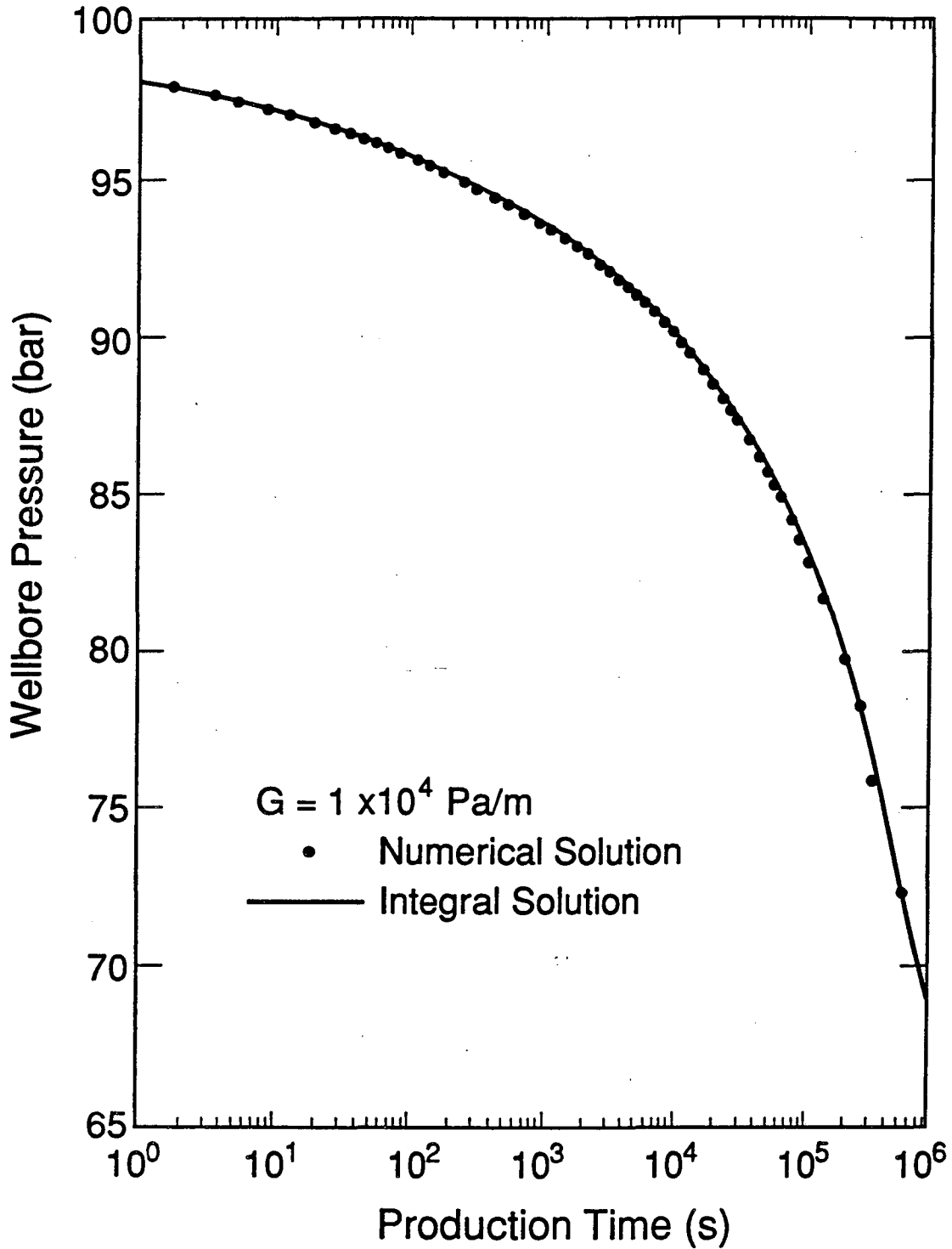
XBL 8911-7881
T.I.D. Illus.88

Figure 1 Comparison of Injection Pressures during Newtonian Fluid Injection, Calculated from the Exact Theis and Integral Solutions.



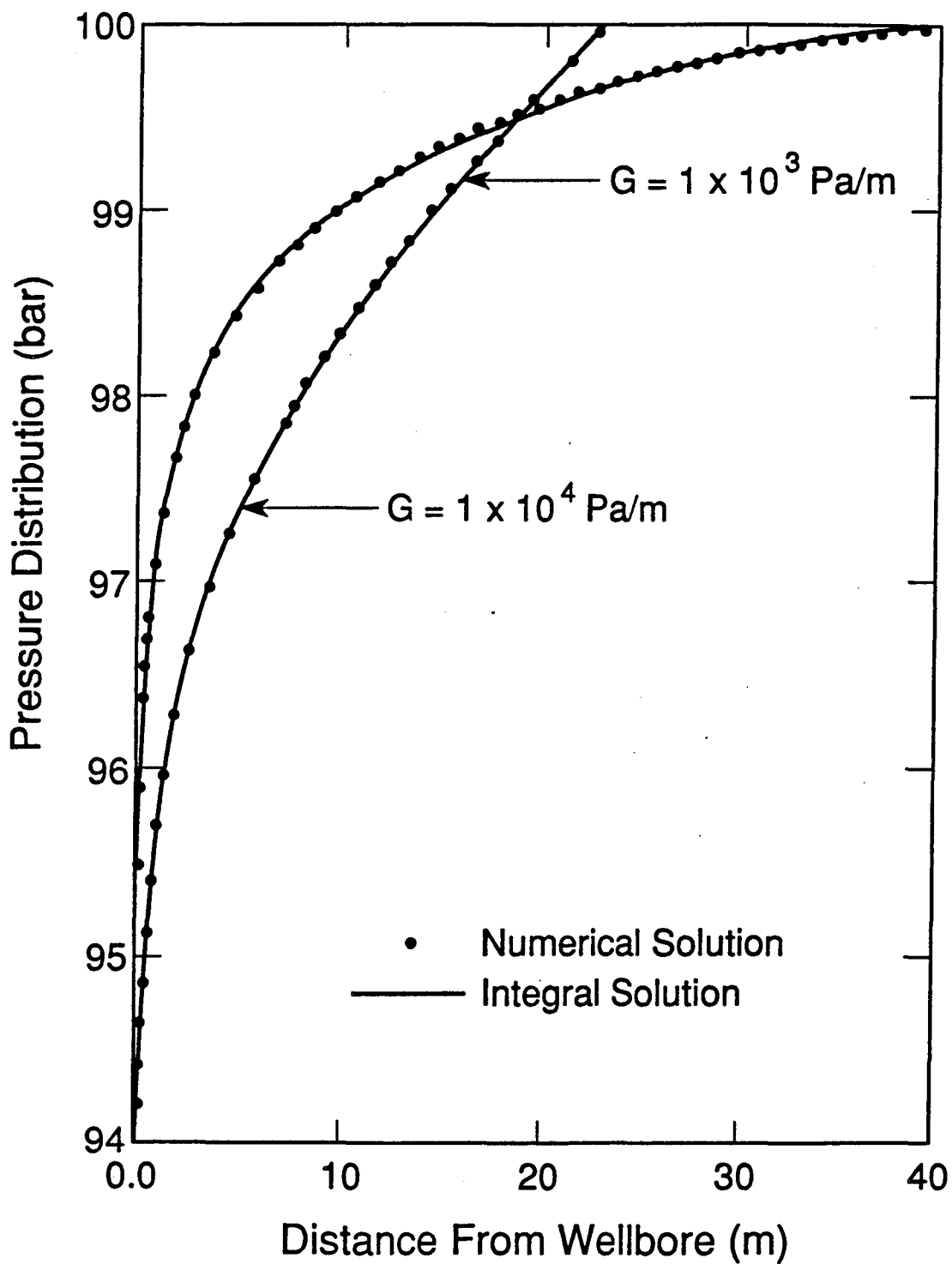
XBL 8911-7882
T.I.D. Illus.88

Figure 2 Comparison of Pressure Distributions of Newtonian Fluid Injection, Calculated from the Exact Theis and Integral Solutions.



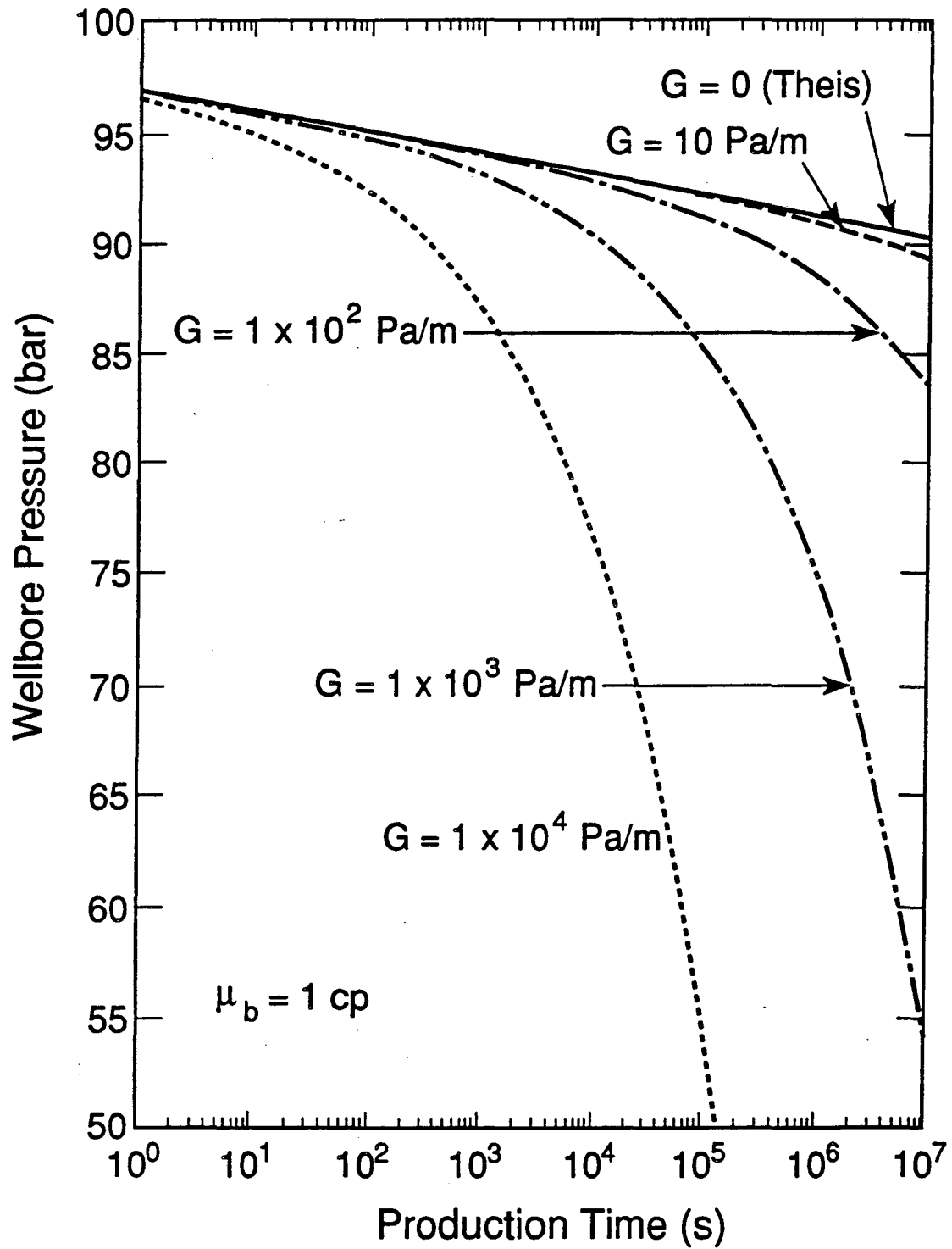
XBL 8911-7885
T.I.D. Illus.88

Figure 3 Comparison of Wellbore Pressures during Bingham Fluid Production, Calculated by the Numerical Simulation and from the Integral Solutions ($C_t = 3 \times 10^{-9} \text{ Pa}^{-1}$, $Q_m = 1 \text{ kg/s}$).



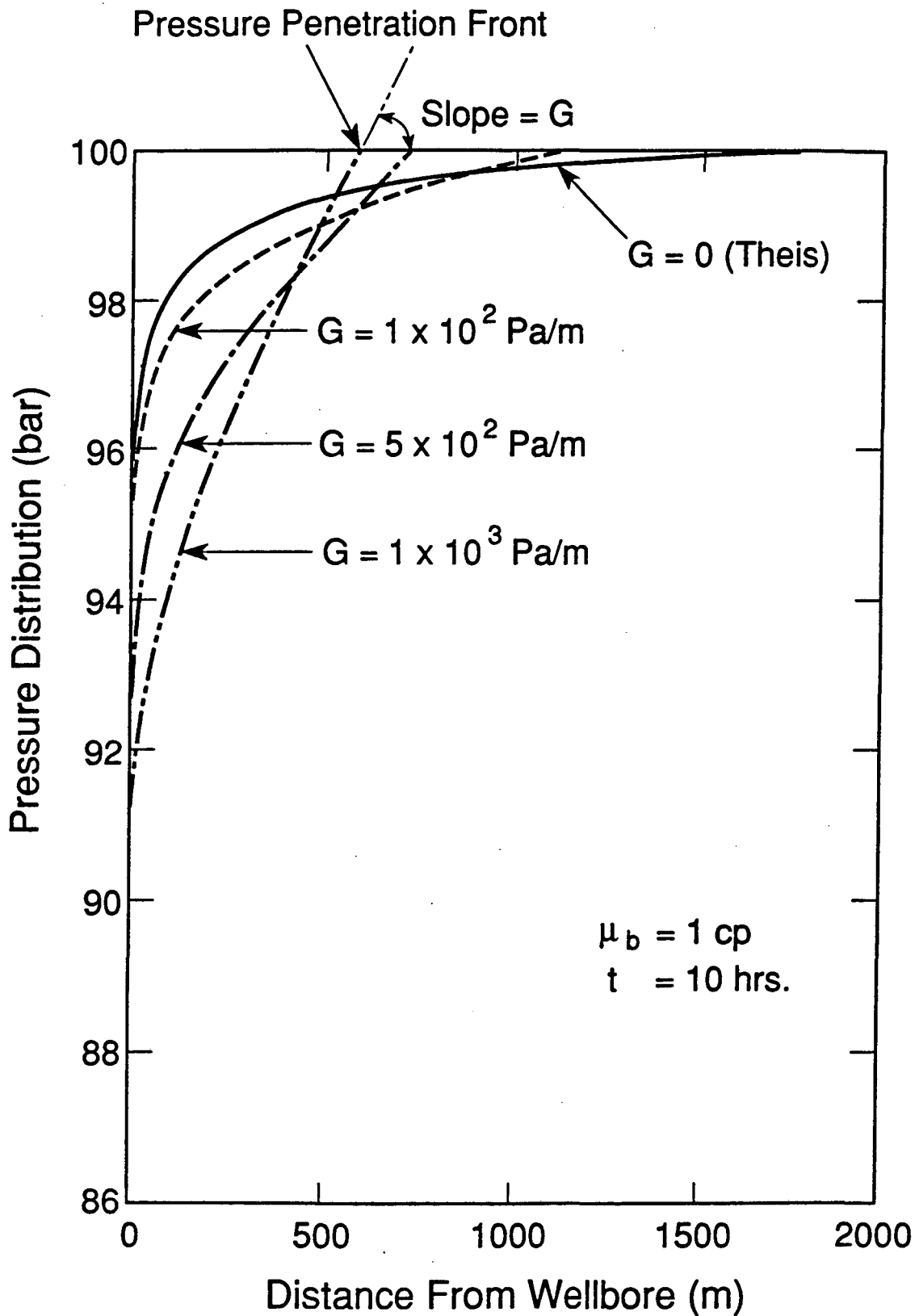
XBL 8911-7886
T.I.D. Illus.88

Figure 4 Comparison of Pressure Distributions of Bingham Fluid Production, Calculated by the Numerical Simulation and from the Integral Solution ($C_t = 3 \times 10^{-9} \text{ Pa}^{-1}$, $Q_m = 1 \text{ kg/s}$).



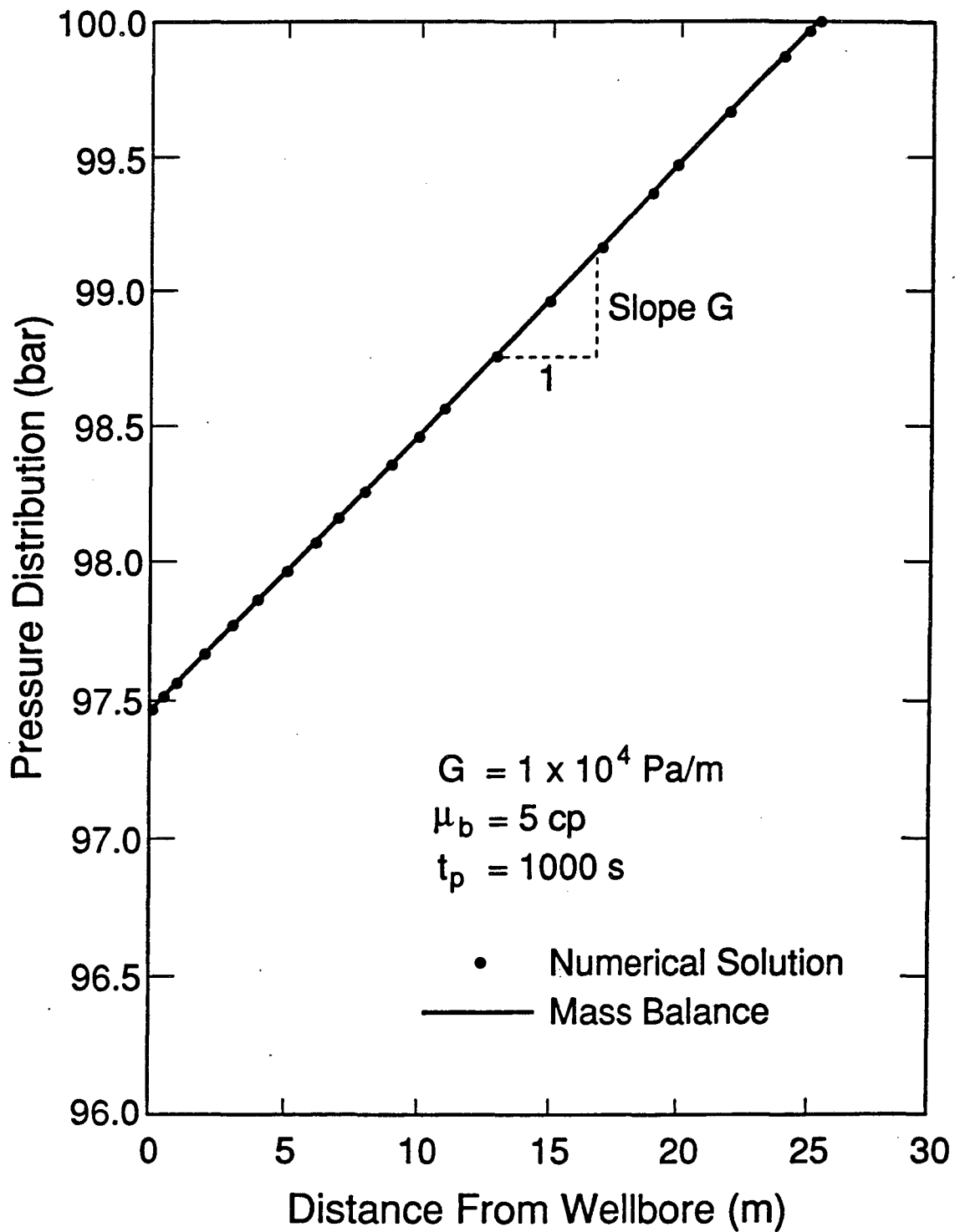
XBL 8911-7887
T.I.D. Illus.88

Figure 5 Transient Wellbore Pressure during Bingham Fluid Production, as Calculated from the Integral Solution, for Different Values of the Minimum Pressure Gradient ($\rho_i = 1000\text{kg/m}^3$, $C_i = 6.56 \times 10^{-10}\text{Pa}^{-1}$, $Q_m = .5\text{kg/s}$).



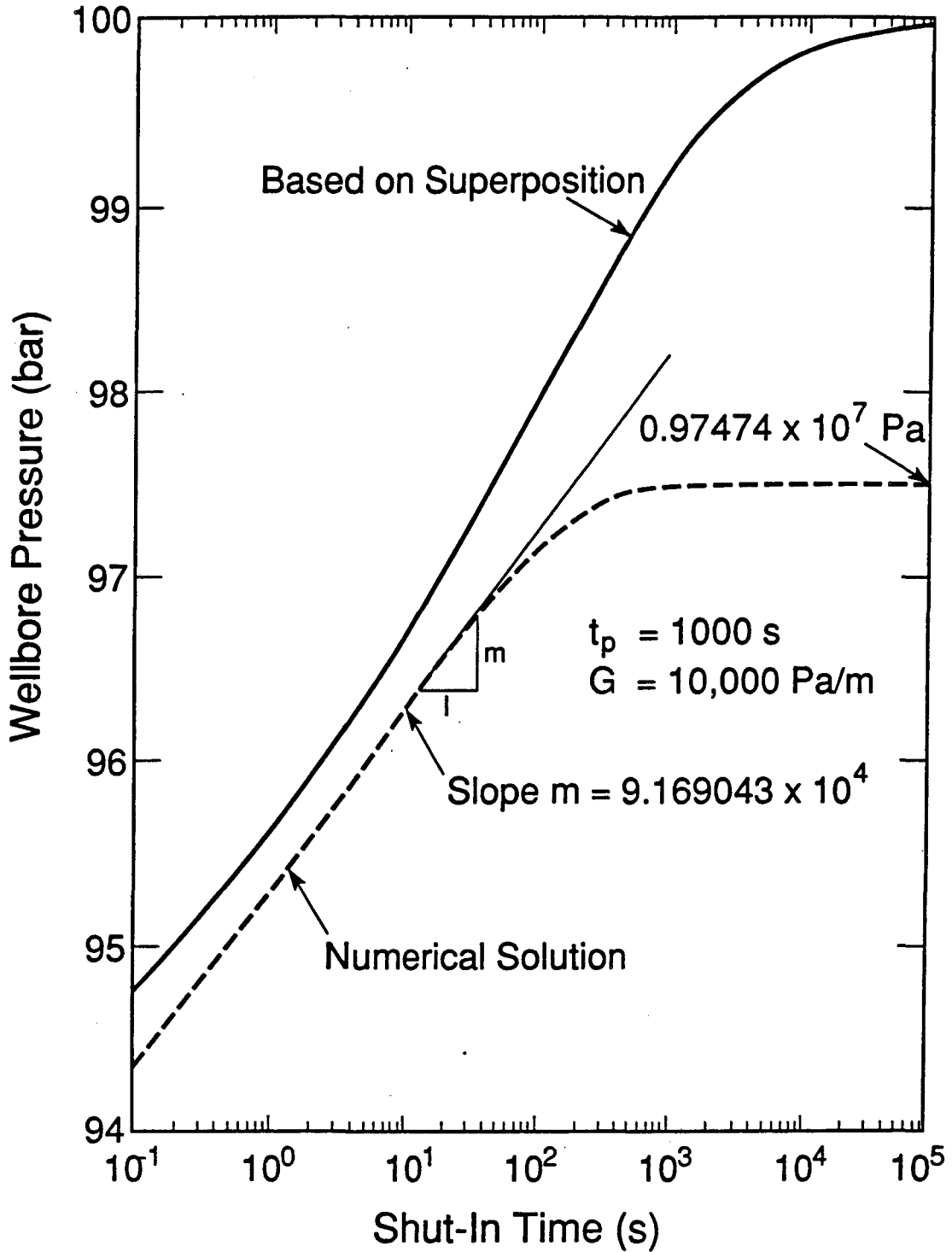
XBL 8911-7888
T.I.D. Illus.88

Figure 6 Pressure Distributions during Bingham Fluid Production, for Different Values of the Minimum Pressure Gradient ($\rho_i = 1000\text{kg/m}^3$, $C_t = 6.56 \times 10^{-10}\text{Pa}^{-1}$, $Q_m = .5\text{kg/s}$).



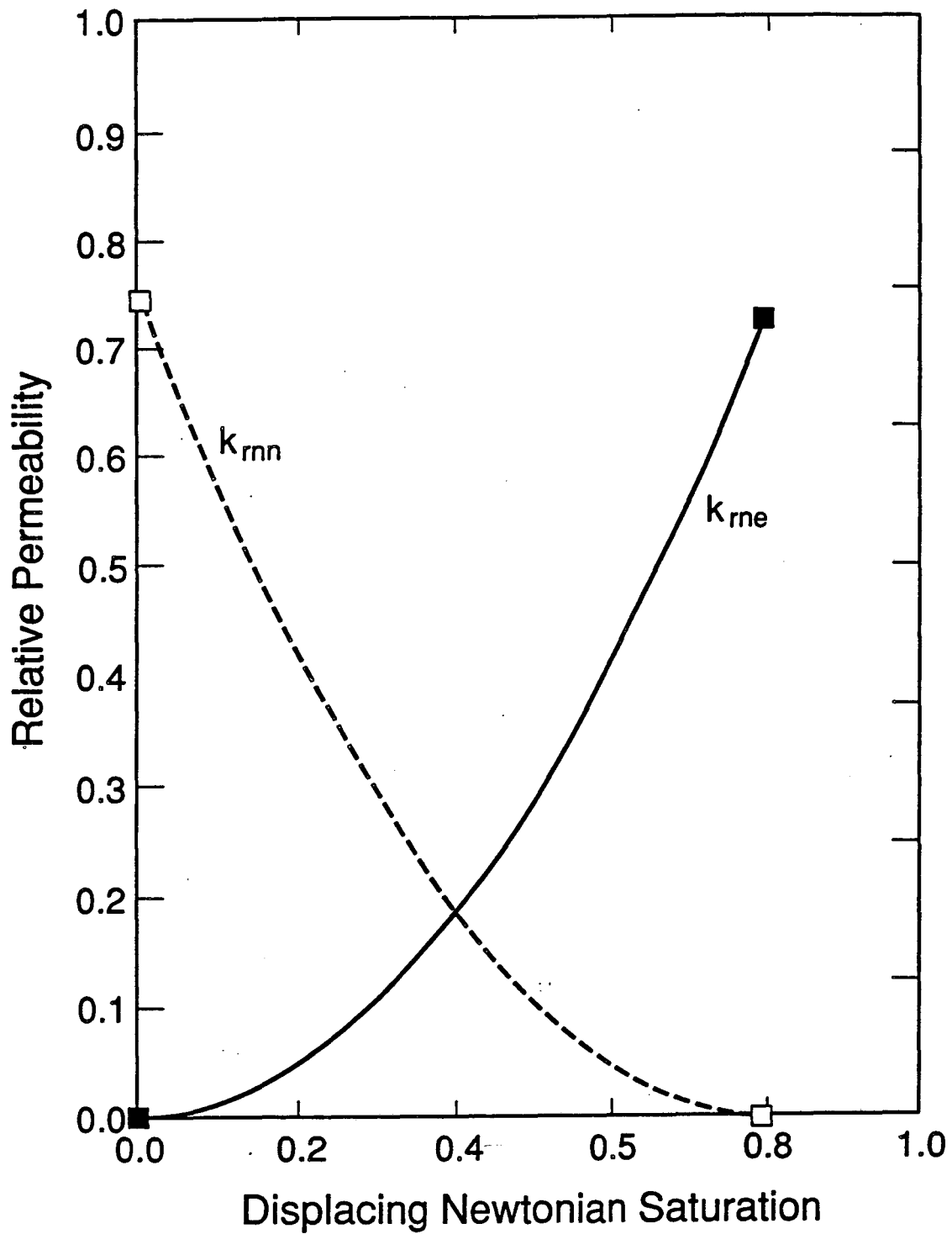
XBL 8911-7892
 T.I.D. illus.88

Figure 7 Pressure Distribution at Long Shut-in Time, Following 1000 Seconds of Bingham Fluid Production ($\mu_b = 5 \times 10^{-3} \text{ Pa}\cdot\text{s}$, $C_t = 9.0 \times 10^{-9} \text{ Pa}^{-1}$, $Q_m = .1 \text{ kg/s}$).



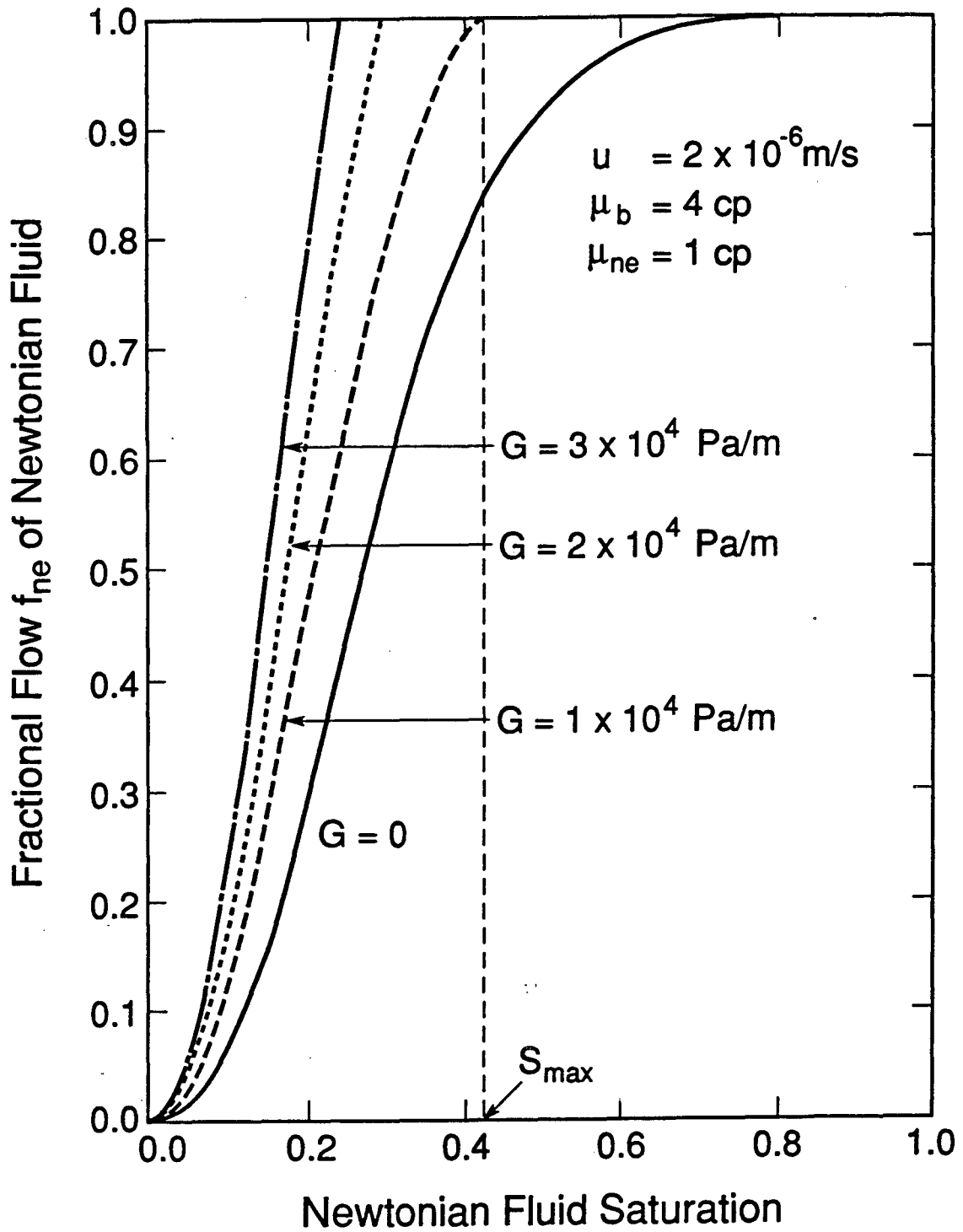
XBL 8911-7895
 T.I.D. illus.88

Figure 8 Numerically Simulated Pressure Buildup during Well Shut-in after 1000 Seconds of Bingham Fluid Production ($\mu_b = 5 \times 10^{-3} \text{ Pa}\cdot\text{s}$, $C_t = 9.0 \times 10^{-9} \text{ Pa}^{-1}$, $Q_m = .1 \text{ kg/s}$).



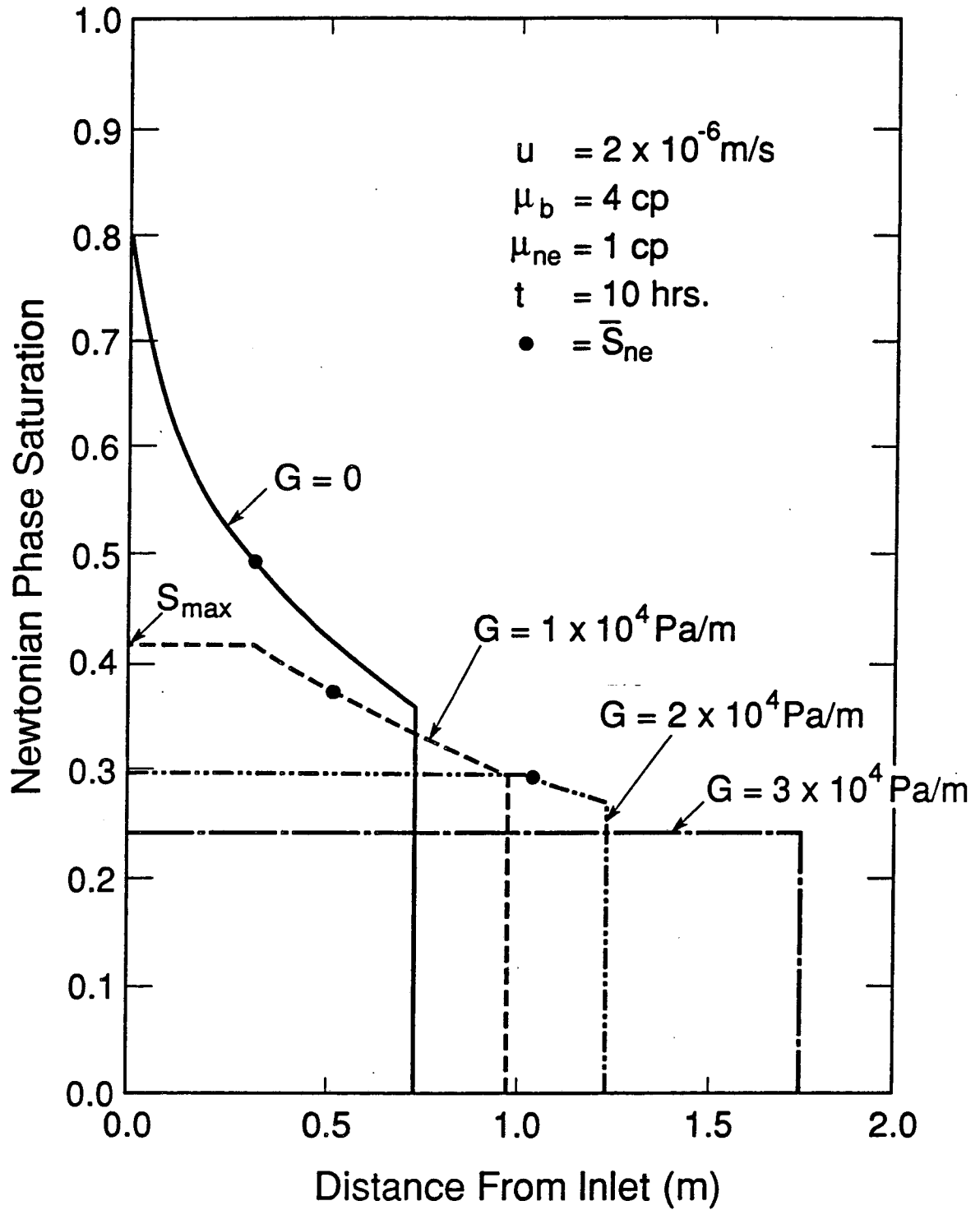
XBL 8911-7860
T.I.D. illus.88

Figure 9 Relative Permeability Functions Used for Evaluation of Displacement of a Bingham Fluid.



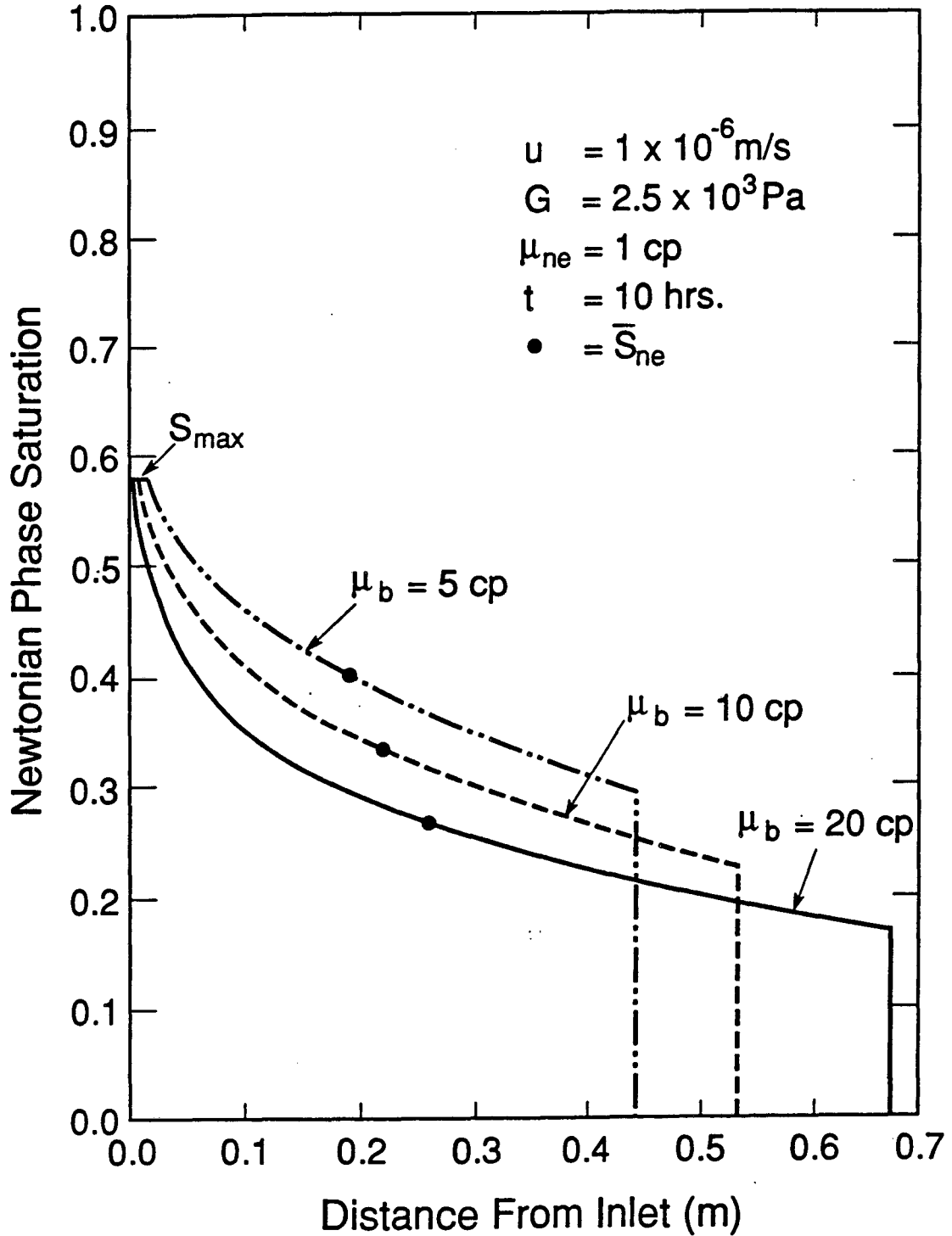
XBL 8911-7863
T.I.D. Illus. 88

Figure 10 Fractional Flow Curves for a Bingham Fluid Displaced by a Newtonian Fluid, for Different Minimum Pressure Gradients.



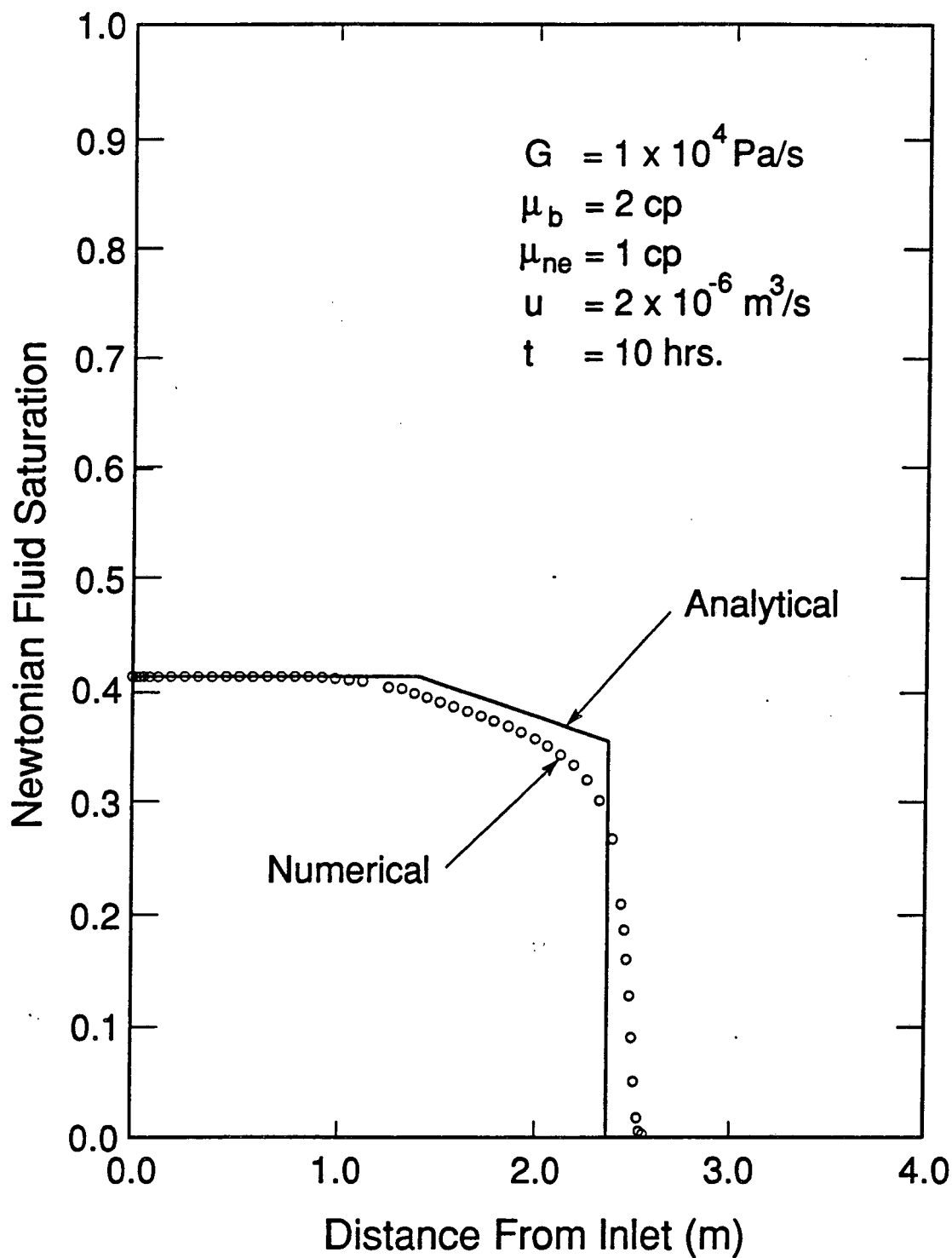
XBL 8911-7865A
T.I.D. Illus.88

Figure 11 Newtonian Phase Saturation Distributions, for Different Values of the Minimum Pressure Gradient of a Bingham Fluid.



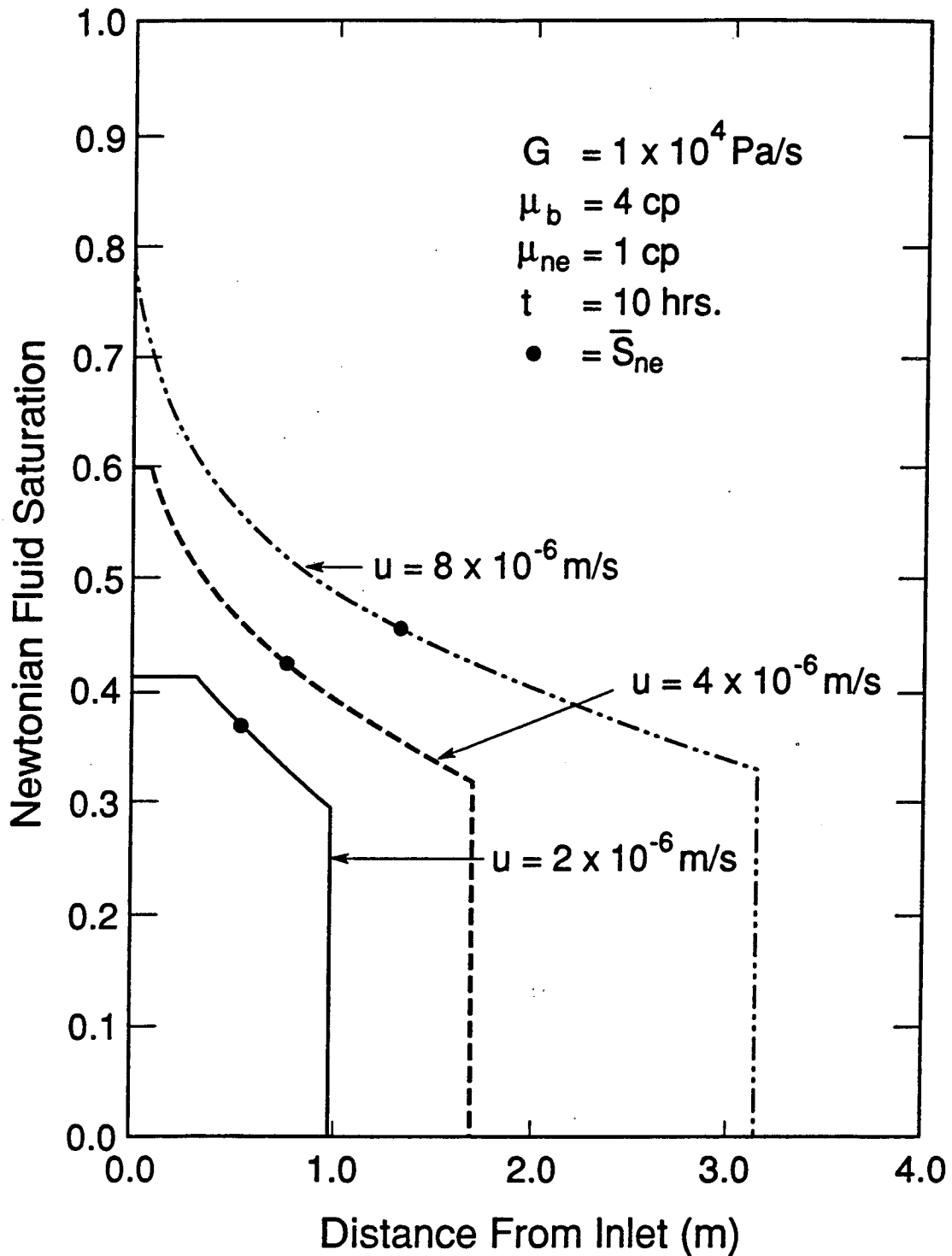
XBL 8911-7868A
T.I.D. Illus.88

Figure 12 Newtonian Phase Saturation Distributions, for Different Values of the Bingham Coefficient μ_b .



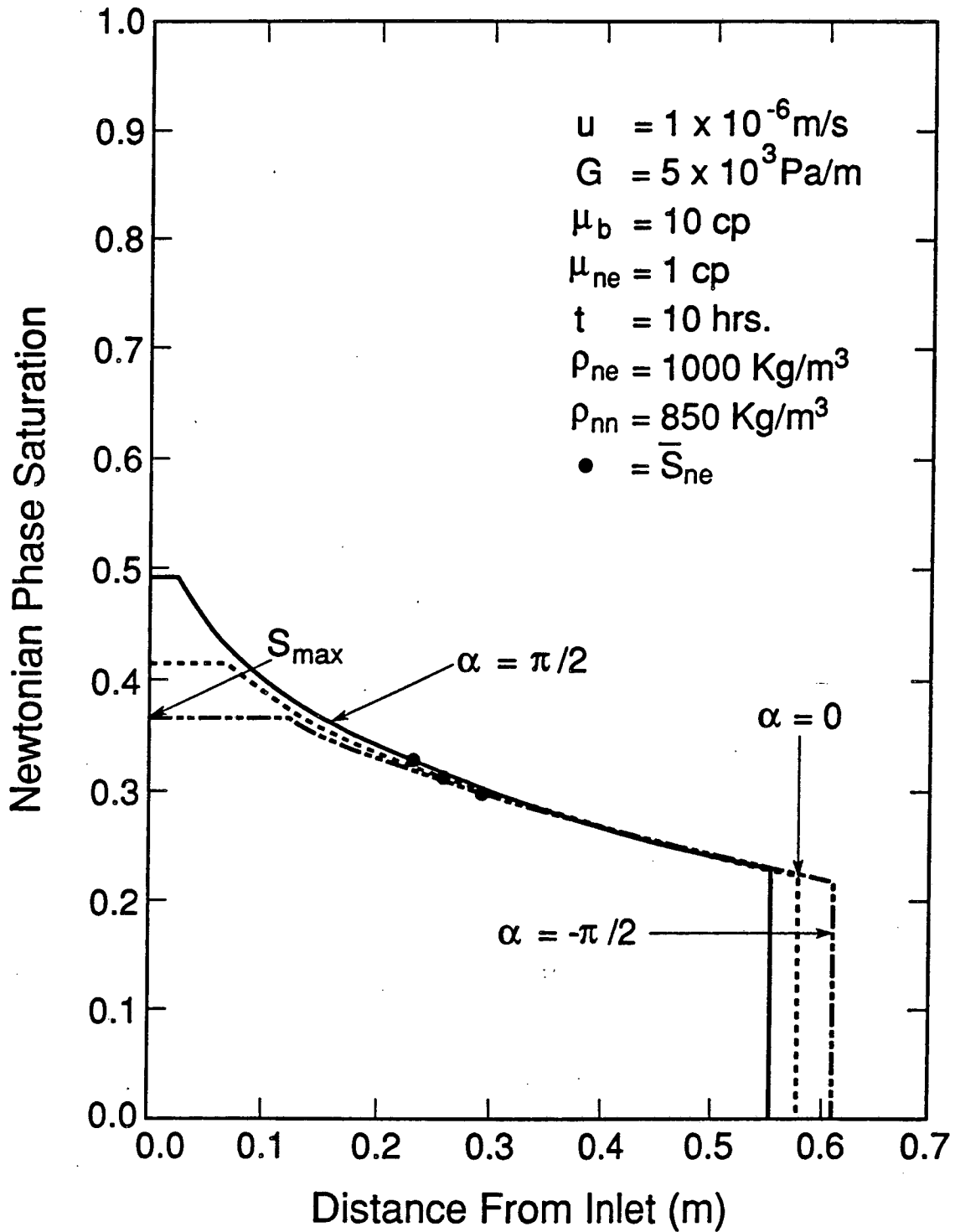
XBL 901-5701
T.I.D. Illus.88

Figure 13 Comparison of Numerical and Analytical Solutions for Two-Phase Immiscible Displacement of a Bingham Fluid by a Newtonian Fluid.



XBL 8911-7874A
T.I.D. Illus.88

Figure 14 Newtonian Phase Saturation Distributions, for Different Injection Rates of a Newtonian Fluid, Displacing a Bingham Fluid.



XBL 8911-7876A
T.I.D. Illus. 88

Figure 15 Newtonian Phase Saturation Distributions for Bingham Fluid Displacement by a Newtonian Fluid with Gravity Effects.

LAWRENCE BERKELEY LABORATORY
TECHNICAL INFORMATION DEPARTMENT
1 CYCLOTRON ROAD
BERKELEY, CALIFORNIA 94720